



Self-Assembly of Symmetrical and Asymmetrical Alkyl Esters in the Neat State and in Oleogels

Gilda Avendaño-Vásquez, Anaïd De la Peña-Gil, María E. Charó-Alvarado, Miriam A. Charó-Alonso and Jorge F. Toro-Vázquez*

Facultad de Ciencias Químicas-CIEP, Universidad Autónoma de San Luis Potosí, San Luis Potosí, Mexico

OPEN ACCESS

Edited by:

Miguel Cerqueira,
International Iberian Nanotechnology
Laboratory (INL), Portugal

Reviewed by:

Vânia Regina Nicoletti,
São Paulo State University, Brazil
Fabio Valoppi,
University of Helsinki, Finland

*Correspondence:

Jorge F. Toro-Vázquez
toro@uaslp.mx

Specialty section:

This article was submitted to
Sustainable Food Processing,
a section of the journal
Frontiers in Sustainable Food Systems

Received: 09 April 2020

Accepted: 24 July 2020

Published: 11 September 2020

Citation:

Avendaño-Vásquez G, De la
Peña-Gil A, Charó-Alvarado ME,
Charó-Alonso MA and
Toro-Vázquez JF (2020)
Self-Assembly of Symmetrical and
Asymmetrical Alkyl Esters in the Neat
State and in Oleogels.
Front. Sustain. Food Syst. 4:132.
doi: 10.3389/fsufs.2020.00132

Saturated alkyl esters play an important role in determining the functional properties of the vegetable waxes used in the formulations of natural cosmetics and edible oleogels. We studied the relationship between the thermo-mechanical properties and crystal microstructure developed by saturated symmetrical (SE: 14:14, 16:16, 18:18, 20:20, and 22:22) and asymmetrical (AE: 18:14, 18:16, 18:20, 18:22) esters in the neat state and in oleogels. Additionally, we evaluated the effect of 1-stearoyl-glycerol (MSG; 0.5 and 1%) in the development of SE and AE oleogels. The X-ray and microscopy analysis in the neat state showed that SE self-assembled developing plate-like crystals, while AE developed acicular-like crystals. Microscopy analysis indicated that AE and SE followed similar crystallization behavior in the oleogels. The AE oleogels had higher elasticity (G') than the SE oleogels. In both types of oleogels as the ester carbon number increased the oleogels' G' decreased and crystal size increased. The addition of just 0.5% MSG, particularly in the AE oleogels, limited the decrease in G' as the ester carbon number increased, mainly because MSG decreased crystal size. The calorimetry results suggested that during cooling the MSG and the alkyl esters developed a co-crystal. Nevertheless, part of the MSG did not interact with the ester molecules and crystallized independently. These MSG crystals acted as active fillers of the microstructure formed by the co-crystals. The overall effect was that in comparison with the alkyl ester oleogels the alkyl ester oleogels with 0.5 and 1% MSG had higher G' with frequency independent rheological behavior. This rheological behavior was particularly evident with the AE oleogels. Therefore, ester composition and molecular structure (i.e., symmetry or asymmetry) greatly influence its molecular self-assembly and subsequently the oleogels' thermo-mechanical properties. Studies using molecular mechanics modeling are underway to establish the mechanism for AE and SE self-assembly with and without MSG. The overall goal is to understand and control the crystallization of vegetable waxes for the development of functional edible oleogels.

Keywords: oleogels, alkyl esters, monoglycerides, vegetable wax, cosmetics, co-crystals

INTRODUCTION

Several molecules of low molecular weight (<3,000 Da) at temperatures below their solubility limit in an organic solvent (i.e., vegetable oil), have the capability of self-assembly. Through this process lipophilic or amphiphilic molecules like phytosterols (Bot and Agterof, 2006; Bot et al., 2008, 2009), lecithin (Han et al., 2014; Martínez-Ávila et al., 2019), monoglycerides (Chen et al., 2009; López-Martínez et al., 2014), (R)-12-hydroxystearic acid (Rogers and Marangoni, 2008; Lam and Rogers, 2011; Abraham et al., 2012; Co and Marangoni, 2013), *n*-alkanes, long chain alkyl esters, fatty acids and fatty alcohols (Gandolfo et al., 2004; Morales-Rueda et al., 2009; Lam and Rogers, 2011; Co and Marangoni, 2013; Sagiri et al., 2015) form three-dimensional crystal structures that physically trap vegetable oils providing them with viscoelastic and thermoreversible properties (Toro-Vazquez and Pérez-Martínez, 2018).

Several studies have shown that this process (i.e., organogelation) is a useful and novel alternative to structure vegetable oils for food systems without the use of *trans* and/or saturated fats (Dassanayake et al., 2011; Marangoni and Garti, 2011; Co and Marangoni, 2012; Rogers et al., 2014). Nowadays, the food industry faces the need to develop thermodynamically stable systems with functional properties accepted by the consumers without the use of *trans* and saturated fatty acids. This is due to the well-documented negative effect of the saturated and *trans* fats on cardiovascular health. One of the most promising alternatives for the development of edible gelled systems (i.e., oleogels) is the use of natural vegetable waxes (Blake et al., 2018). Additionally, the major cosmetic companies are moving away from animal-based (e.g., tallow) and petroleum derived materials (e.g., petroleum jelly), looking now for renewable and functional vegetable-based materials. We can also develop vegetable waxes-based oleogels with useful and novel functional properties for the cosmetics' industry (Ferrari and Mondet, 2003; Morales et al., 2010; Perez-Nowak, 2012). The use of vegetable waxes is the current natural trend for the development of natural cosmetics, e.g., organic cosmetics (Cosmetic Lab, 2016; Fórmula Botánica, 2019).

Most of the vegetable waxes already in the commercial market are characterized by their high content of long chain saturated alkyl esters (i.e., >60%). In other waxes a different lipid-like compound is the major component (i.e., *n*-alkanes) and the alkyl esters is a minor but still a significant component fraction (between 6 and 16%) (Blake et al., 2018). In any case, the alkyl esters in the vegetable waxes are essentially constituted by saturated long chain fatty acids between 16 and 32 carbon atoms (Doan et al., 2017), which provide the waxes with a solid texture at room temperature. Exception to this is the liquid wax obtained from jojoba (*Simmondsia chinensis*) seeds composed by nearly 97% of esters constituted by heneicosanoic acid (21:0), behenic acid (22:0), and particularly 13, 16-docosadienoic acid (22:2), and fatty alcohols of 20, 22 and 24 carbons with one double bond (*cis*-11-eicosenol, *cis*-13-docosenol, and *cis*-15-tetracosenol) (Busson-Breyse et al., 1994; Ghamdi et al., 2017). Thus, the alkyl ester content is often used to explain

the crystallization and melting behavior of the vegetable waxes in the neat state and in the development of oleogels. Within this context, rice bran and sunflower waxes are considered chemically homogeneous given their high alkyl ester content (92–100%) and low compositional heterogeneity (i.e., less than 6% of free alkyl acids and free alkyl alcohols) (Doan et al., 2017). These two vegetable waxes crystallize as one single narrow exotherm, developing large needle-like crystals with high melting entropy values. In contrast, carnauba and candelilla wax with lower concentration of their main component (i.e., carnauba wax with 62–85% of alkyl esters and candelilla wax with 45–65% of *n*-alkanes) have higher heterogeneous composition. In consequence, the carnauba and the candelilla wax crystallize showing broader exotherms with multiple peaks developing small dendritic crystals or microplatelets, respectively, with lower melting entropy. This is particularly evident with candelilla wax that shows the higher compositional heterogeneity with just 6–16% of alkyl esters (Alvarez-Mitre et al., 2012; Blake et al., 2014; Doan et al., 2017).

From the above, it is evident that the alkyl esters play an important role in the physical properties showed by vegetable waxes. Nevertheless, there is limited information about their physical properties either in the pure state or in oleogels. Within this context the main objective of this study was to investigate the relationship between the thermomechanical properties and crystal microstructure developed by saturated alkyl esters in the neat state and in oleogels. This, using pure alkyl esters constituted by saturated fatty acids and fatty alcohols with the same number of carbons [symmetrical esters; myristyl myristate (14:14), palmityl palmitate (16:16), stearyl stearate (18:18), arachidyl arachidate (20:20) and behenyl behenate (22:22)] and with different number of carbon [asymmetrical esters; stearyl myristate (18:14), stearyl palmitate (18:16), stearyl arachidate (18:20), and stearyl behenate (18:22)].

On the other hand, studies done by different research groups had shown that the crystallization behavior of vegetable waxes (i.e., crystal size and shape) and further development of the crystal network are affected by other components, naturally present in the wax or intentionally added (Toro-Vazquez et al., 2007; Dassanayake et al., 2009; Morales-Rueda et al., 2009; Chopin-Doroteo et al., 2011; Blake et al., 2014; Hwang et al., 2014; Rocha-Amador et al., 2014). Monoglycerides are a minor component commonly present in refined vegetable oils at low concentrations commonly between 0.05 and 0.2% (Gunstone, 2002). Because their amphiphilic character and capability of developing hydrogen bonds when added to vegetable oils the monoglycerides are able to develop emulsions and oleogels (Ojijo et al., 2004; Chen et al., 2009; López-Martínez et al., 2014; Marangoni and Garti, 2018). Therefore, monoglycerides play an important role in the development and stability of organogelled emulsions (Toro-Vazquez et al., 2013a). In these systems the monoglycerides might affect the self-assembly of alkyl esters present in vegetable waxes. Thus, a second objective of this study was to investigate the effect of intentionally added monoglycerides (0.5 and 1%) in the self-assembly of alkyl esters during the formation of oleogels.

MATERIALS AND METHODS

Materials

Refined, bleached and deodorized high oleic safflower oil was obtained from a local distributor (Coral International, San Luis Potosi, Mexico). The high oleic safflower oil was used as the liquid phase in the development of oleogels. As previously determined by HPLC the major triacylglyceride in the vegetable oil was OOO ($65.65 \pm 0.15\%$), followed by LOO ($16.26\% \pm 0.04$), and POO ($8.58\% \pm 0.04$), and minor concentrations of StOO ($2.64 \pm 0.01\%$), LLO ($2.25 \pm 0.02\%$), POL ($1.70\% \pm 0.11$), StLL ($0.87 \pm 0.05\%$), and LLL ($0.46 \pm 0.01\%$) (O = oleic acid; L = linoleic acid; St = stearic acid; P = palmitic acid) (Alvarez-Mitre et al., 2012). Analytical grade 1-stearoyl-*rac*-glycerol (MSG) with a purity >99% was obtained from Sigma Aldrich (St. Louis, MO, USA). The linear alkyl esters with a purity > 99% were obtained from Nu-Check Prep, Inc. (Elysian, MN, USA) and were constituted by saturated fatty acids and saturated fatty alcohols with the same number of carbons (i.e., symmetrical esters, SE) or with different number of carbon (i.e., asymmetrical esters, AE). The SE were: tetradecyl tetradecanoate (myristyl myristate; 14:14), hexadecyl hexadecanoate (palmityl palmitate; 16:16), octadecyl octadecanoate (stearyl stearate; 18:18), eicosyl eicosanoate (arachidyl arachidate; 20:20), and docosanyl docosanoate (behenyl behenate; 22:22), and the AE were: octadecyl tetradecanoate (stearyl myristate; 18:14), octadecyl hexadecanoate (stearyl palmitate; 18:16), octadecyl eicosanoate (stearyl arachidate; 18:20), and octadecyl docosanoate (stearyl behenate; 18:22). The MSG and alkyl esters were stored under desiccant conditions (phosphorus pentoxide) at -20°C .

X-Ray Measurements

Neat alkyl esters were initially heated at 160°C for 20 min, after that the samples were allowed to cool at room temperature followed by 24 h storage at -5°C . After this time the samples X-ray pattern, in a silicon crystal sample holder, were recorded at 5°C with a Bruker D8 Advance diffractometer (CuK α -irradiation $\lambda = 1.5406$, high-rate detector Lynx Eye) equipped with a parallel beam geometry. Angular scans were obtained from 1° to 40° using a step size of 0.01° and a scan speed of $0.32^\circ/\text{s}$. Data processing and analyses were performed using DIFFRAC.EVA software (V 5.1, Bruker, Karlsruhe, Germany).

Crystallization and Melting Behavior of Alkyl Esters

Differential Scanning Calorimetry of Neat Alkyl Esters

The crystallization and melting profile of the neat alkyl esters (SE and AE) were determined by differential scanning calorimetry (Q2000, TA Instruments; New Castle, DL, USA). The corresponding sample ($\approx 5\text{--}7$ mg) was sealed in aluminum pans, heated at 160°C for 20 min and then cooled to $10^\circ\text{C}/\text{min}$ until achieving -5°C . After 2 min at this temperature the system was heated at $5^\circ\text{C}/\text{min}$ until achieving 160°C . The use of this time-temperature condition assured the full melting of all the alkyl esters studied, particularly those with the highest number of carbons (i.e., 20:20, 22:22). The crystallization and heating thermograms were determined with the equipment

software by plotting the heat flux of the sample as a function of the temperature. Using the first derivative of the heat flux from the cooling thermogram we determined the temperature at the beginning of the crystallization exotherm (T_{Cr}), and the area below the corresponding exotherm (i.e., heat of crystallization; ΔH_{Cr}). From the heating thermogram we determined the temperature at the maximum of the heat flow of the endotherm (T_M), and the heat of melting (ΔH_M). For each alkyl ester we obtained two independent cooling and heating thermograms ($n = 2$).

Fitting of the Hildebrand Equation

We evaluated the ideal crystallization/melting behavior of the SE and AE through the Hildebrand equation (Hildebrand and Robert-Lane, 1950),

$$\ln(x) = \frac{\Delta H_M}{R \left(\frac{1}{T_S} - \frac{1}{T_E} \right)} \quad (1)$$

$$\frac{1}{T_S} = \frac{1}{T_E} + \frac{R[\ln(X)]}{\Delta H_M} \quad (2)$$

where ΔH_M is the enthalpy of fusion per mole of the corresponding neat alkyl ester, T_E and T_S are the melting temperature of the neat alkyl ester and in the oil solutions (i.e., $T_S = T_M$; see previous section), respectively, X is the mole fraction of the alkyl ester in the vegetable oil, and R is the universal gas constant. For this we prepared 500 mg of 0.5–5% alkyl esters solutions in safflower oil solutions in glass vials (12 mm \times 35 mm). To solubilize the alkyl esters the vials were placed in an oven set to 100°C and heated during 15 min with intermittent 1 min gently mixing periods using a vortex mixer. The crystallization and heating thermograms for the alkyl esters solutions in safflower oil as described in previous section. However, in this case the sample was heated at 100°C for 20 min and then cooled to $10^\circ\text{C}/\text{min}$ until achieving -5°C . After 2 min at this temperature the system was heated at $5^\circ\text{C}/\text{min}$ until achieving 100°C . The corresponding thermal parameters were fitted to the Hildebrand equation determining the linear regression of $\ln(X)$ on $1/T_S$ and comparing the ΔH_M for neat alkyl esters calculated with the fitting equation with the corresponding ΔH_M value determined experimentally. For each alkyl ester concentration of the SE and AE we did at least three independent determinations ($n \geq 3$).

Effect of MSG in the Thermal Behavior of Alkyl Esters Solutions in the Vegetable Oil

To evaluate the MSG effect in the crystallization/melting behavior of the alkyl esters, we prepared 3% alkyl esters-MSG solutions containing 0, 0.5, or 1% (wt/wt) of MSG. For this we prepared the corresponding 3% alkyl ester solution as indicated in the previous section, adding the corresponding proportion of MSG once the alkyl esters solution achieved $80\text{--}85^\circ\text{C}$. Afterwards, the alkyl ester and alkyl ester-MSG solutions were stored at 5°C until their use. The crystallization and melting profile of the 3% alkyl esters-MSG solution were determined by differential scanning calorimetry. To evaluate the MSG effect in the crystallization and

melting profile of the alkyl ester-MSG system, we determined also the cooling and heating thermograms for the 0.5 and 1% MSG solutions in safflower oil. For each of the alkyl esters-MSG systems studied we obtained two independent cooling and heating thermograms ($n = 2$).

Rheological Measurements in the Oleogels

The storage (G') and loss (G'') modulus of the alkyl ester-MSG systems were measured with an Anton Paar MCR301 rheometer (Paar Physica MCR 301, Stuttgart, Germany) using a steel truncated cone plate geometry (CP25-1TG). A sample of a pre-heated ($\approx 100^\circ\text{C}$) alkyl ester-MSG system was applied on the base of the rheometer geometry previously set at 100°C , and the cone was set using the true-gap function of the software. After 20 min at 100°C , the system was cooled at $10^\circ\text{C}/\text{min}$ until achieving -5°C . After 2 min at this temperature we applied a strain sweep between 0.001 and 100% using a frequency (ω) of 1 Hz. The G' and G'' of the alkyl ester-MSG system were obtained from the linear viscoelastic region (strain between 0.002 and 0.03%). In a parallel experiment we determined the phase shift angle (δ) as a function of ω (-5°C ; 100 and 0.1 Hz) using a strain within the linear viscoelastic region. The sample temperature was controlled with a Peltier temperature control located on the base of the geometry and with a Peltier-controlled hood (HPTD 200). The control of the equipment was made through the software Start Rheoplus US200/32 version 2.65 (Anton Paar, Graz, Austria). For each alkyl ester-MSG system we did two independent rheological measurements ($n = 2$).

Polarized Light Microscopy

Polarized light microphotographs (PLM) of the oleogels were obtained using a polarizing light microscope (Olympus BX51; Olympus Optical Co., Ltd., Tokyo, Japan) equipped with a color video camera (KP-D50; Hitachi Digital, Tokyo, Japan) and a heating/cooling stage (TP94; Linkam Scientific Instruments, Ltd., Surrey, England) connected to a temperature control station (LTS 350; Linkam Scientific Instruments, Ltd.) and a liquid nitrogen tank. A drop of the alkyl ester-MSG solution was applied on a glass slide and then set in the heating/cooling stage of the microscope. We applied the same time-temperature program as described in section 2.3, but here after arriving at a temperature 10°C above the corresponding T_{Cr} the sample was smear on the slide surface using another pre-heated glass slide at a 45° angle. Then, the stage was closed and the cooling continued until achieving -5°C . PLM of the corresponding microstructure were obtained after 2 min at this temperature.

Statistical Analysis

The treatment conditions studied (i.e., type of alkyl ester, concentration of MSG) were analyzed by ANOVA and contrast between the treatment means. The corresponding thermal parameters were fitted to the Hildebrand equation by linear regression. In all cases the software used was STATISTICA V 12 (StatSoft Inc., Tulsa, OK).

RESULTS AND DISCUSSION

X-Ray Diffraction and Thermal Behavior of Neat Alkyl Esters

The corresponding lattice spacings (d , Å) and calculated extended molecular lengths (L , Å) for the neat SE and AE are summarized in **Table 1**. As stated in the Materials and Methods section, the SE and AE oleogels studied were developed and characterized at -5°C while the X-ray analysis of the neat alkyl esters was done at 5°C . Unfortunately the diffractometer could not control the temperature below 5°C . However, as determined by DSC, the melting of the neat alkyl esters occurred at temperatures well above 5°C (see further discussion associated to **Figure 3B**). Within this context, we assumed that the alkyl esters' crystal polymorph present at 5°C was the same that at -5°C . The X-ray diffractograms (WAXS and SAXS) for the neat SE and AE are shown in the **Figures 1SM–5SM** of the Supplementary Material. The d value determined in the SAXS region (**Table 1**) was associated with the length of the repetition structural unit formed by the alkyl ester molecules in the crystal. In both type of esters the d values were shorter than the thicknesses of a lamellar structure resulting from two stacked alkyl chain molecules and larger than a single molecule. Unfortunately, we could not find reports in the literature about the molecular organization of neat alkyl esters in the solid state. Within this context, we propose that the SAXS d value resulted of structural units formed by parallel interdigitated alkyl chain molecules, possible with an inclination angle. This organization would allow the stabilization of the structure along the parallel hydrocarbon chains through van der Waals forces and, allegedly through hydrogen bonds developed between the oxygen of the carbonyl group and an alpha hydrogen of the parallel alkyl ester molecule. Preliminary results obtained by our group through molecular mechanics simulations showed that, in addition to intermolecular dispersion forces, the formation of hydrogen bonds between parallel interdigitated alkyl ester molecules might occur between the parallel hydrocarbon chains. Within this framework, the length of the repetition unit determined by X-ray diffraction for the SE showed values of 44.64 Å, 52.02 Å, 62.80 Å, 71.83 Å, and 82.28 Å for the 14:14, 16:16, 18:18, 20:20, and 22:22, respectively; and for the AE of 67.28 Å, 67.28 Å, and 65.21 Å for 18:16, 18:20, and 18:22, respectively (**Table 1**). It was interesting to note that for the SE the length of the repetition unit showed a significant linear relationship with the number of carbons of the alkyl ester ($R^2 = 0.997$, $P < 0.001$). In contrast, for the AE the 18:16, 18:20, and 18:22 had a similar repetition unit length, this despite the increase in the carbon number from 34 (18:16) to 40 (18:22). This behavior was not observed by the 18:14 ester. The 18:14 was the only alkyl ester that showed two short-angle spacings at 43.49 Å and 52.34 Å, indicating that neat 18:14 crystallized in two different polymorphs. We also observed these two 18:14 polymorphs in the corresponding melting thermogram (results show later in **Figure 6SM** panel B). Thus, the polymorphism might be associated with the different behavior of the 18:14 unit length when compared with the mean unit length's observed by 18:16, 18:20, and 18:22 ($66.59 \text{ Å} \pm 1.19 \text{ Å}$). On the other hand, the d values showed by

TABLE 1 | Lattice spacing (d) determined by X-ray diffraction (SAXS and WAXS region) and calculated extended molecular length (L) for the alkyl esters studied in neat powder.

	Alkyl ester	d (Å)		L^a (Å)	Proposed packing arrangement	Predominant crystal shape
		SAXS region	WAXS region			
Symmetric	14:14	44.64	12.43, 4.54, 4.39, 4.30, 4.20, 4.09, 3.80	36.93	Monoclinic	Platelet
	16:16	52.02	14, 15, 4.60, 4.29, 4.21, 4.11, 3.80	42.21	Monoclinic	Platelet
	18:18	62.80	16.01, 4.34, 4.27, 4.21, 4.12, 3.80	47.48	Monoclinic	Platelet
	20:20	71.83	17.79, 4.15, 3.73	52.76	Orthorhombic	Platelet
	22:22	82.28	19.78, 4.23, 3.78	58.03	Orthorhombic	Platelet
Asymmetric	18:14	52.34, 43.49	4.22, 3.80	42.21	Orthorhombic	Acicular
	18:16	67.28	16.97, 4.24, 3.82	44.84	Orthorhombic	Acicular
	18:20	67.28	17.04, 4.23, 3.81	50.16	Orthorhombic	Acicular
	18:22	65.21	16.67, 4.23, 3.77	52.76	Orthorhombic	Acicular

^aThe corresponding alkyl ester molecule was obtained using Chemdraw Ultra software (V. 12.0.2.1076; Cambridge Soft Corporation, USA), and then measured using Chem3D software (V. 17.1). In order to obtain the theoretical carbon-carbon length, in all cases we preserved the extended molecular configuration of the alkyl ester.

the alkyl esters in the WAXS region corresponded to higher order diffractions in the progression shown by a lamella packing arrangement. Thus, the diffractograms for the AE and for 20:20 and 22:22 showed the characteristic d values for an orthorhombic subcell with WAXS diffraction peaks at approximately 3.8 Å and 4.2 Å (Table 1). In contrast, 14:14, 16:16, and 18:18 did not show a diffraction pattern that supported their assignation to a particular subcell structure (Table 1). Nevertheless, similar to neat n -alkanes that crystallize in the monoclinic subcell structure, the major diffraction peak for these alkyl esters appeared at 4.2 Å. Thus, the neat 14:14, 16:16, and 18:18 were tentatively associated to a monoclinic subcell structure. We also observed that except 16:16, the relative intensity of the SE diffractograms was weaker in the SAXS region than in the WAXS region (Figures 1SM–3SM; Supplementary Material). This difference in the diffraction intensity was higher the longer the alkyl chains of the SE. These results showed that the molecular interactions within the lamellar planes (i.e., interplanar short spacings) of SE crystals occurred more frequently than those between the parallel interdigitated alkyl chain molecules. The parallel interdigitated chain molecules were aligned along the axis vertical to the interplanar plane (i.e., long spacings). The overall result was that, except 16:16, the neat SE crystals had a lower growth along the axis perpendicular to the lamellar plane in comparison with the interplanar growth. Consequently, we might expect that neat SE crystallized developing mainly plate-like crystals. In contrast, the AE diffractograms showed a lower diffraction signal in the WAXS region than in the SAXS region (Figures 4SM, 5SM; Supplementary Material). Therefore, the neat AE crystallized along the axis vertical to the interplanar plane, thus developing mainly acicular-like crystals. Unfortunately, PLM photographs of neat alkyl esters were very difficult to obtain. This, mainly because under the experimental conditions neat esters crystallized very fast overcrowding the field and making impossible to distinguish crystals' shape and size. Within this context we decided to evaluate the crystal shape developed by the alkyl esters using concentrated vegetable oil solutions (60% wt/wt). We assumed that at this high concentration the effect of minor components

or the triacylglycerides of the vegetable oil did not affect the crystallization habit of the alkyl esters of that occurring in the neat state. The PLM for the 60% solutions for some AE (i.e., 18:14 and 18:20) and SE (i.e., 16:16 and 20:20) are shown in Figures 1, 2. In the 60% ester solutions the 18:14 and 18:20 developed fibrillar crystals while the 16:16 and 20:20 formed plate crystals. These results showed that the symmetry or asymmetry of the alkyl ester had an effect in the crystal shape.

The crystallization and melting thermograms for the neat AE and SE are shown in Figure 6SM (Supplementary Material), and the T_{Cr} , T_M , ΔH_{Cr} , and ΔH_M behavior as a function of the ester's carbon number are shown in Figures 3, 4. Using low molecular weight gelators in the neat state and in vegetable oil solution, our group established that the gelator's molecular structure is associated with the onset of their molecular self-assembly (i.e., T_{Cr}) (Toro-Vazquez et al., 2013b). In the same way we established that the gelator's solubility temperature in the vegetable oil is indirectly associated with T_{Cr} , while T_M and the heats of melting (ΔH_M) and crystallization (ΔH_{Cr}) are associated with the energies of the molecular interactions that stabilize the crystal structure in the neat state and in the oleogel (Toro-Vazquez et al., 2013b). Within this context, independent of the type of alkyl ester (i.e., SE or AE), T_{Cr} and T_M of the neat alkyl esters had a direct linear relationship with the carbon number ($P < 0.005$; Figure 3). The linear equations reported in Figures 3A,B indicated that the increase of just one carbon in the alkyl chain of SE and AE resulted in a T_{Cr} and T_M increment of about 2°C. In other words, independent of the type of ester, the longer the ester hydrocarbon chain the higher the onset temperature for its molecular self-assembly (i.e., higher T_{Cr}). In the same way, the longer the alkyl ester the higher the temperature to achieve the complete breakup of the non-covalent interactions stabilizing the alkyl ester crystals (i.e., higher T_M). Similar results for T_M have been reported for neat n -alkanes with even and odd carbon number between 7 and 32 (Boese et al., 1999; McGann and Lacks, 1999). These results showed that T_{Cr} and T_M of the alkyl esters in the neat state depend essentially on the carbon number. Consequently, the longer the alkyl esters chain the higher the onset temperature

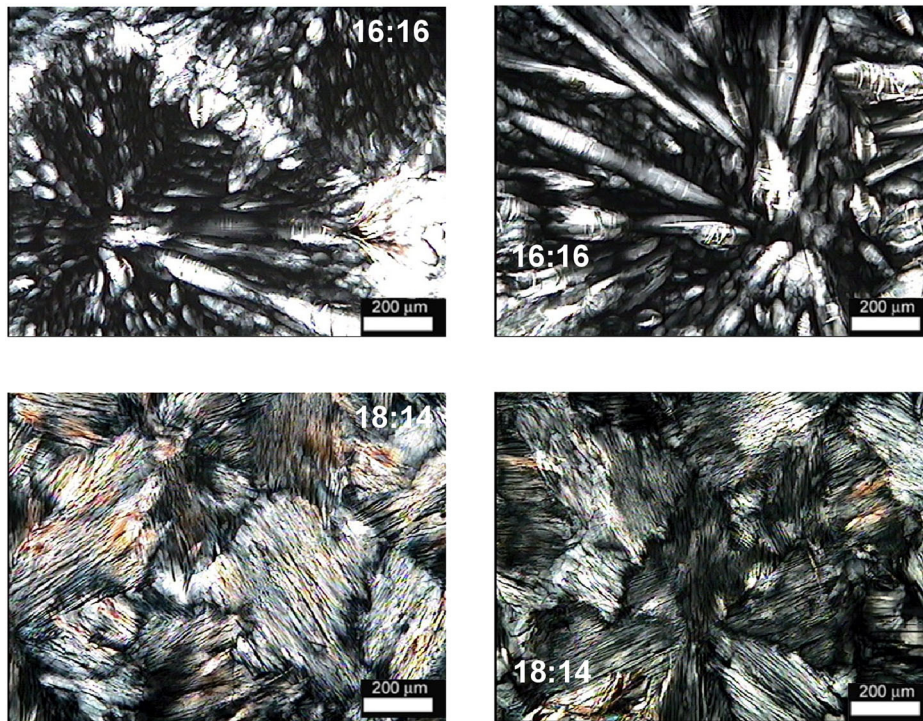


FIGURE 1 | Polarized light microscopy for 60% (wt/wt) solutions in high oleic safflower oil of the symmetric (16:16) and asymmetric (18:14) alkyl esters. The same ester solution is presented for two preparation slides at the same level of magnification.

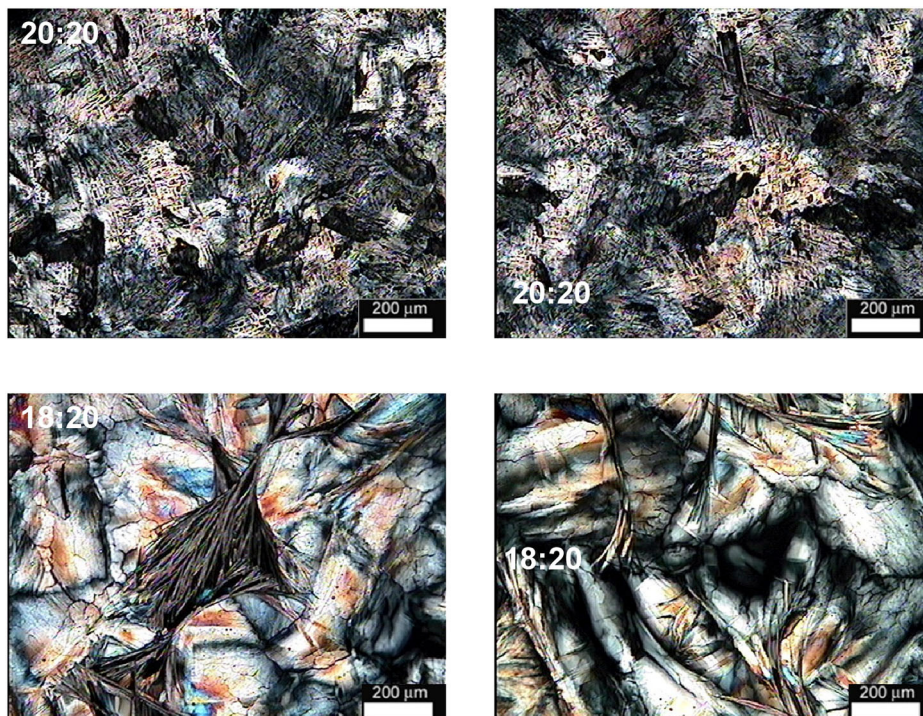


FIGURE 2 | Polarized light microscopy for 60% (wt/wt) solutions in high oleic safflower oil of the symmetric (20:20) and asymmetric (18:20) alkyl esters. The same ester solution is presented for two preparation slides at the same magnification.

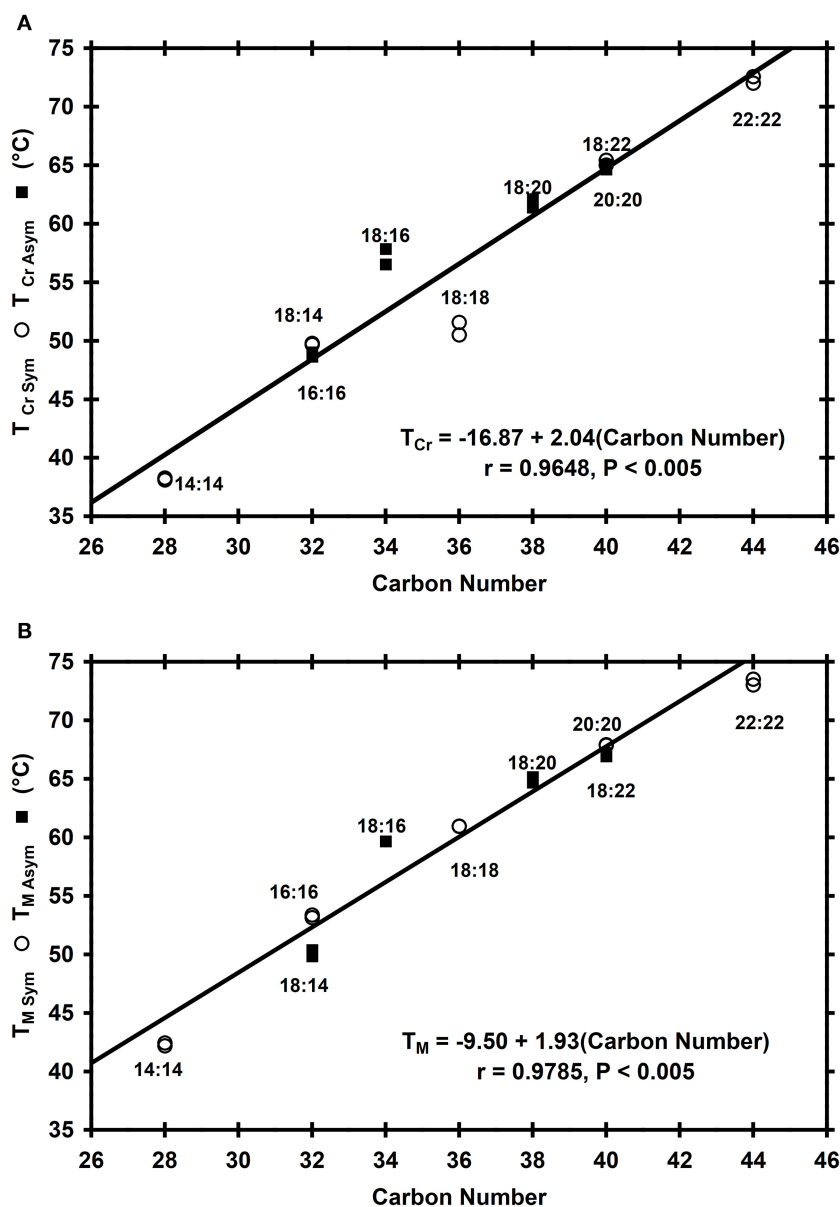


FIGURE 3 | Crystallization (T_{Cr}) and melting (T_M) temperatures for the neat symmetric and asymmetric neat esters as a function of the carbon number of the alkyl esters. The equations show the linear regression of T_{Cr} (**A**) and T_M (**B**) as a function of the alkyl esters carbon number, the corresponding regression coefficient (r) and statistical significance (P).

for the molecular self-assembly (i.e., T_{Cr}) and more significant the van der Waals forces became for molecular self-assembly and crystal structure stabilization (i.e., higher T_M). The results shown in **Figure 3** showed that the symmetry or asymmetry of the alkyl esters studied did not affect the T_{Cr} and T_M behavior as a function of the carbon number.

On the other hand, in comparison with T_{Cr} and T_M the ΔH_{Cr} and ΔH_M of the neat alkyl esters showed a different behavior as a function of the carbon number (**Figure 4**). Thus, ΔH_{Cr} and ΔH_M for the SE observed a quadratic increase as a function of the carbon number ($R^2 > 0.89$; $P < 0.001$). In contrast, for the

AE the 18:16, 18:20, and 18:22 showed statistically the same ΔH_{Cr} and ΔH_M with mean values of 141.5 kJ/mol (± 7.4 kJ/mol) and 138.0 kJ/mol (± 7.7 kJ/mol), respectively. However, of all AE studied 18:14 showed the lower ΔH_{Cr} (109.7 ± 4.2 kJ/mol) and ΔH_M (107.2 ± 6.3 kJ/mol) values, a behavior surely associated with its polymorphic behavior as established previously by X-ray analysis (**Figure 4SM** panel A; Supportive Information). The 18:14 polymorphic behavior was also observed in the corresponding melting thermogram as one minor endotherm around 38°C followed by a major endotherm around 49°C (**Figure 6SM** panel B). The ΔH_M plotted for 18:14 in **Figure 4B**

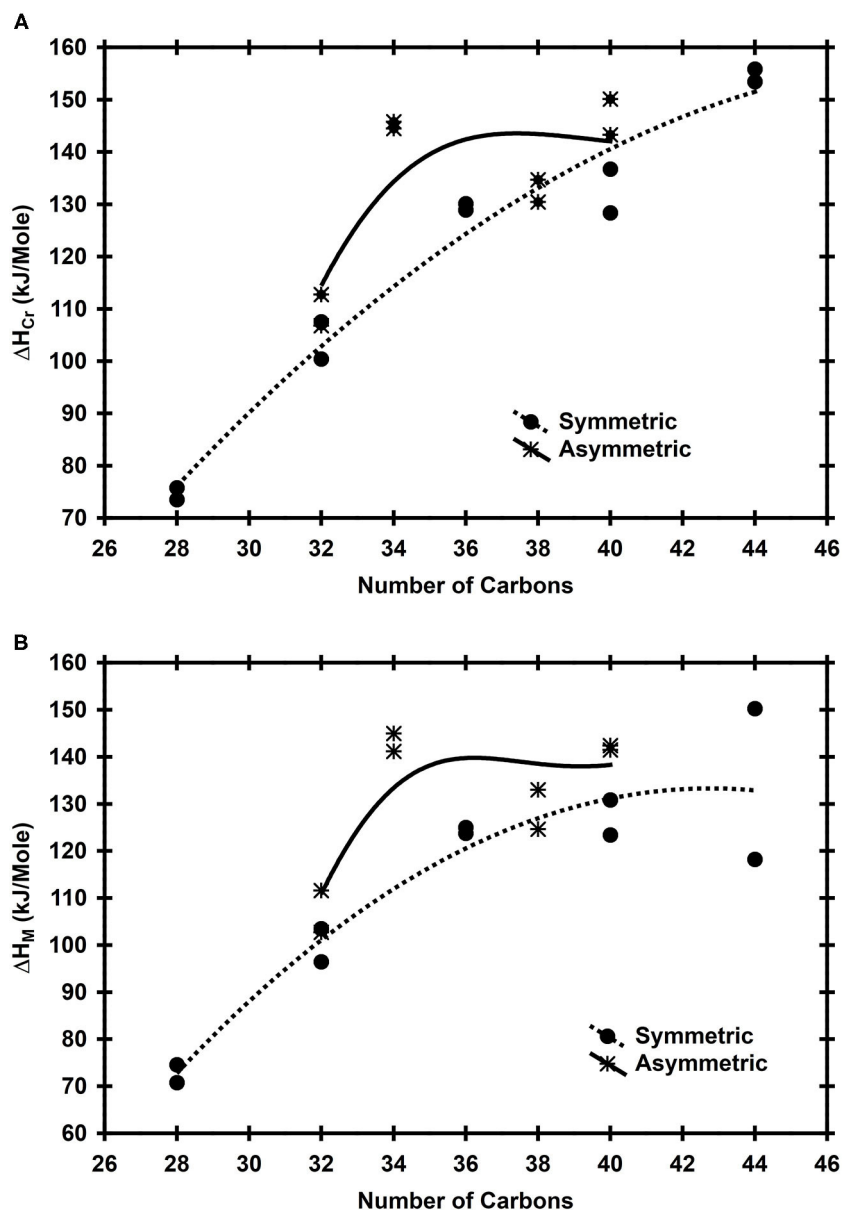


FIGURE 4 | Heat of crystallization [ΔH_{Cr} ; (A)] and melting [ΔH_M ; (B)] for the neat symmetric and asymmetric esters as a function of the alkyl esters carbon number.

was just for the major exotherm. Thus, the lower ΔH_{Cr} , ΔH_M , and shorter length of the repetition unit of 18:14 (Table 1; Figure 4) were the result of its polymorphism. Thus, ΔH_{Cr} and ΔH_M for the AE followed a similar trend as the repetition unit length previously discussed, i.e., 18:16, 18:20, and 18:22 had the same repetition unit length ($66.59 \text{ \AA} \pm 1.19 \text{ \AA}$) while 18:14 showed two short-angle spacings at 43.49 \AA and 52.34 \AA . These results along with the X-ray diffractograms (Figures 1SM–5SM) and PLM (Figures 1, 2) observations showed that the symmetry or asymmetry of the ester molecules had a significant effect in the crystallization of neat esters. We also observed an additional difference in the crystallization behavior between SE and AE.

It is well established that supercooling, i.e., the difference between the melting and the crystallization temperature of a compound, provides the thermodynamic drive for the molecular self-assembly of gelator molecules. Thus, from the corresponding thermograms of each ester we calculated the difference between the temperature at the end of melting (T_{M-End}) and the onset temperature for crystallization (T_{Cr-O}). Within this context, the difference $T_{M-End} - T_{Cr-O}$ for the ester solutions was considered as a relative measurement of the supercooling required to achieve the alkyl ester crystallization. The Figure 7SM showed that the relative supercooling required to achieve the molecular self-assembly of AE increased linearly ($R^2 = 0.78$; $P < 0.10$) as

a function of the carbon number while for SE decreased ($R^2 = 0.80$; $P < 0.05$). Thus, as the carbon number increased the molecular self-assembly of the AE was harder to achieve than for the SE (**Figure 7SM**). However, the energy required for melting (ΔH_M) of the orthorhombic crystals developed by 18:16, 18:20, and 18:22 was statistically the same (**Figure 4B**). This, in spite of the increase in the carbon number for these AE. In contrast, the energy required for melting of the SE crystals increased quadratically as a function of the carbon number (**Figure 4B**), achieving a plateau above 40 carbons (20:20). Above a carbon number of 40 the SE crystallized in the orthorhombic phase while below 40 carbons (i.e., 14:14, 16:16, and 18:18) as monoclinic (**Table 1**). Based on the supercooling behavior shown in **Figure 7SM**, the crystal shape and polymorph developed by alkyl esters would depend on their symmetry or asymmetry and in their length.

Behavior of the Asymmetric and Symmetric Esters in Vegetable Oil Solution

We used the Hildebrand equation (Equation 1) to fit the corresponding thermal parameters obtained with the 0.5–5% (wt/wt) ester oil solutions. With the cooling program used 14:14 solutions below 3% did not achieve full crystallization. Therefore, to have enough experimental data just for the 14:14 ester we included the 6% ester concentration. The results showed that for all ester solutions the Hildebrand equation (Equation 2) fitted the change of T_s (i.e., melting temperature of the alkyl ester in the oil solution, T_M) as a function of the ester molar fraction with a determination coefficient (R^2) above 0.90 ($P < 0.01$). The Hildebrand equation parameters for the AE and SE solutions in vegetable oil and corresponding statistical significance of the linear regression are reported in **Table 1SM** of the Supplementary Material. These results showed that within the concentration interval used for the AE and SE solutions (**Table 1SM**), the alkyl esters behave as ideal solutes in the vegetable oil, i.e., the melting temperature of the AE and SE in the vegetable oil was a direct function of the alkyl ester concentration.

Within the previous context we used the corresponding Hildebrand equation (**Table 1SM** of the Supplementary Material) to estimate the ΔH_M and T_M values for the neat AE and SE assuming an X value of 1 (i.e., ΔH_M and T_M were the estimated values for the neat esters). Subsequently, we determined the percentage of absolute error when these values were used as predictors of the corresponding experimental ΔH_M and T_M values. The results showed that, independent of the type of ester, the predicted T_M had an absolute error lower than 9%. In contrast, the predicted ΔH_M for the neat SE had an absolute error between 15 and 51%. On the other hand, except the equation for 18:14 that provided an absolute error of 18%, the predicted ΔH_M for the neat AE had an absolute error lower than 9%. Evidently, the SE developed a different crystal organization (i.e., polymorph) crystallizing from the vegetable oil solution than from the melt, and from there the large differences observed between the predicted and the experimental ΔH_M value. In contrast, except 18:14, the AE in vegetable oil solutions and from the melt crystallized developing the same polymorph (i.e.,

orthorhombic; **Table 1**). As already discussed, 18:14 was the only ester that showed the development of two polymorphs, a phenomenon probably associated to the low predictive capacity of the estimated ΔH_M value. Unfortunately, we could not corroborate these conclusions with experimental measurements since at the ester concentration used in the vegetable oil (i.e., lower than 6%), the X-ray signal of our equipment was low and did not provide reliable diffractograms.

Relationship Between the Rheology and Microstructure of the Asymmetric and Symmetric Esters Oleogels

The development of an oleogel requires the formation of a self-supporting structure by the gelator's molecules that physically trap the organic solvent. The minimal gelling concentration of a gelator (i.e., vegetable wax, alkyl ester), also known as the critical gelling concentration, is associated to the minimal mass of crystals that develops the self-supporting structure in a giving solvent (i.e., vegetable oil). This gelling parameter is function of the gelator solubility in the solvent as affected by time-temperature conditions (i.e., gel setting temperature, cooling rate) (Toro-Vazquez and Pérez-Martínez, 2018). Thus, the minimal gelator concentration for vegetable waxes with significant concentration of alkyl esters (e.g., carnauba wax, rice hull wax, safflower wax) has been reported between 1 and 5% by different authors (Dassanayake et al., 2009; Blake et al., 2014; Patel et al., 2015). However, there are not minimal or critical gelator concentration data reported in the literature for neat alkyl esters in vegetable oil or any other solvent. Unfortunately, because limited availability of pure esters, we could not experimentally determine their minimal gelator concentration. Working with n -alkanes with 24, 28, 32, and 36 carbons and several organic solvents, Abdallah and Weiss (2000) reported critical gelator concentrations $>5.1\%$, $>2.1\%$, 2.3% , and 1.3% , respectively. In the same way, using silicon oil, mineral oil and decane as solvents Pal et al. (2013) reported critical gelator concentrations between 0.6 and 3.8% for a series of positional isomers of keto octadecanoic acid (i.e., carboxylic acids with a carbonyl group inserted in different positions). However, none of these studies used vegetable oil as solvent. Thus, we established a 3% (wt/wt) ester concentration to compare the thermo-mechanical properties of AE and SE oleogels with and without MSG. As already mentioned, the monoglycerides are minor native components present in vegetable oils. However, once intentionally added to the vegetable oil to develop emulsions or organogelled emulsions, their amphiphilic character and capability of developing hydrogen bonds might favor or hinder the self-assembly of the alkyl esters.

The G' , measured at -5°C , as a function of the carbon number for the 3% AE and SE oleogels with 0, 0.5, and 1% of MSG are shown in **Figure 5**. As established by DSC, at -5°C we assured the complete crystallization of the alkyl ester and MSG present in the vegetable oil solutions. The PLM photographs for the corresponding SE oleogels with 0, 0.5, and 1% MSG are shown in **Figures 6–8** and for the AE oleogels in **Figures 9–11**. Independent of the MSG concentration we achieved the highest

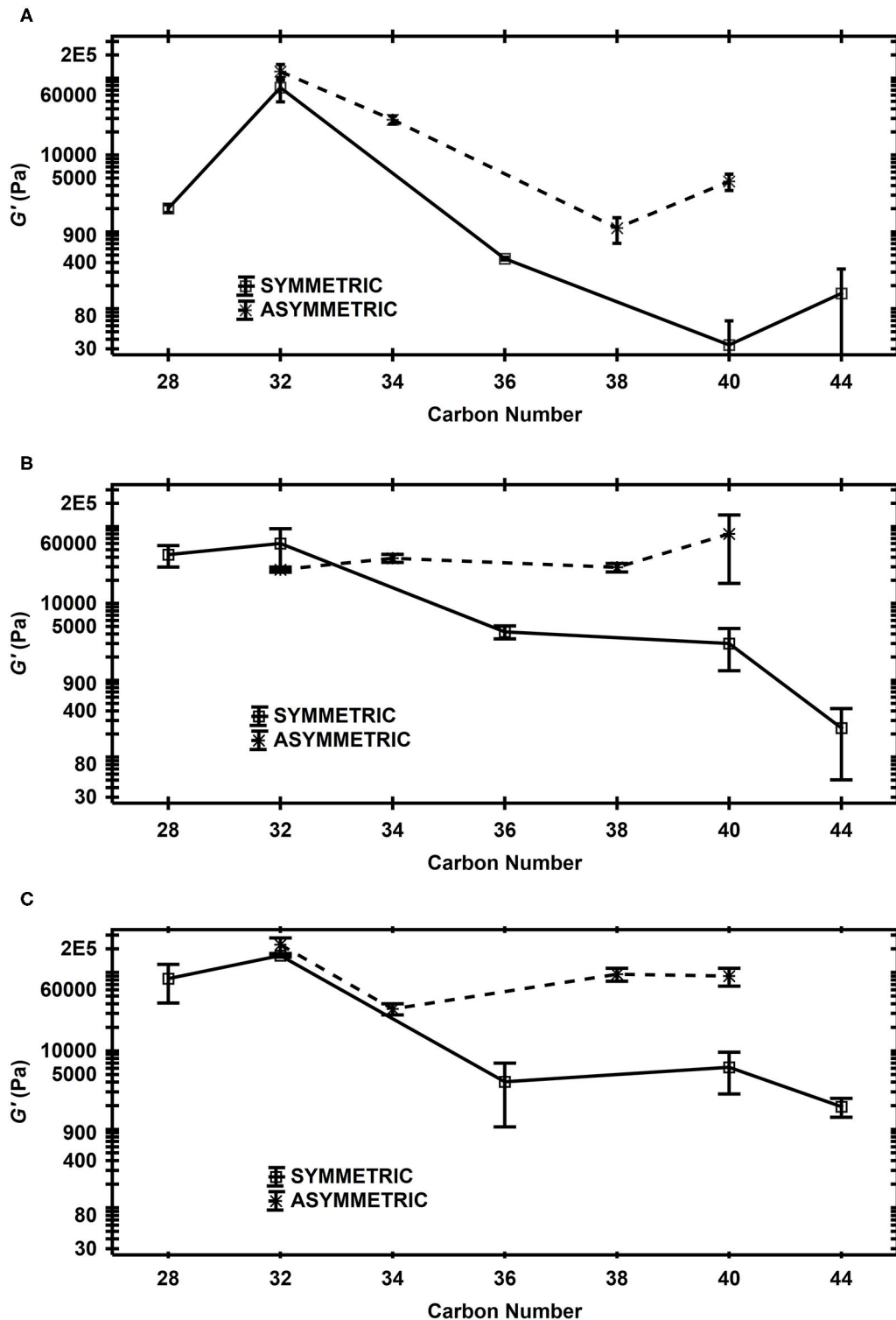


FIGURE 5 | Elastic modulus (G' ; -5°C) for the 3% (wt/wt) oleogels formulated with symmetric and asymmetric alkyl esters as a function of the carbon number of the esters. **(A)** 0% MSG; **(B)** 0.5% MSG; **(C)** 1% MSG (wt/wt).

oleogel's elasticity in the AE and SE oleogels developed with the 32 carbons esters (i.e., 16:16 and 18:14; $P < 0.05$) (Figure 5). Above 32 carbons, independent of the MSG concentration, the

elasticity of the SE oleogels showed a decreasing trend as the carbon number increased (Figure 5). The AE oleogels with 0% MSG also showed a similar G' decreasing behavior (Figure 5A).

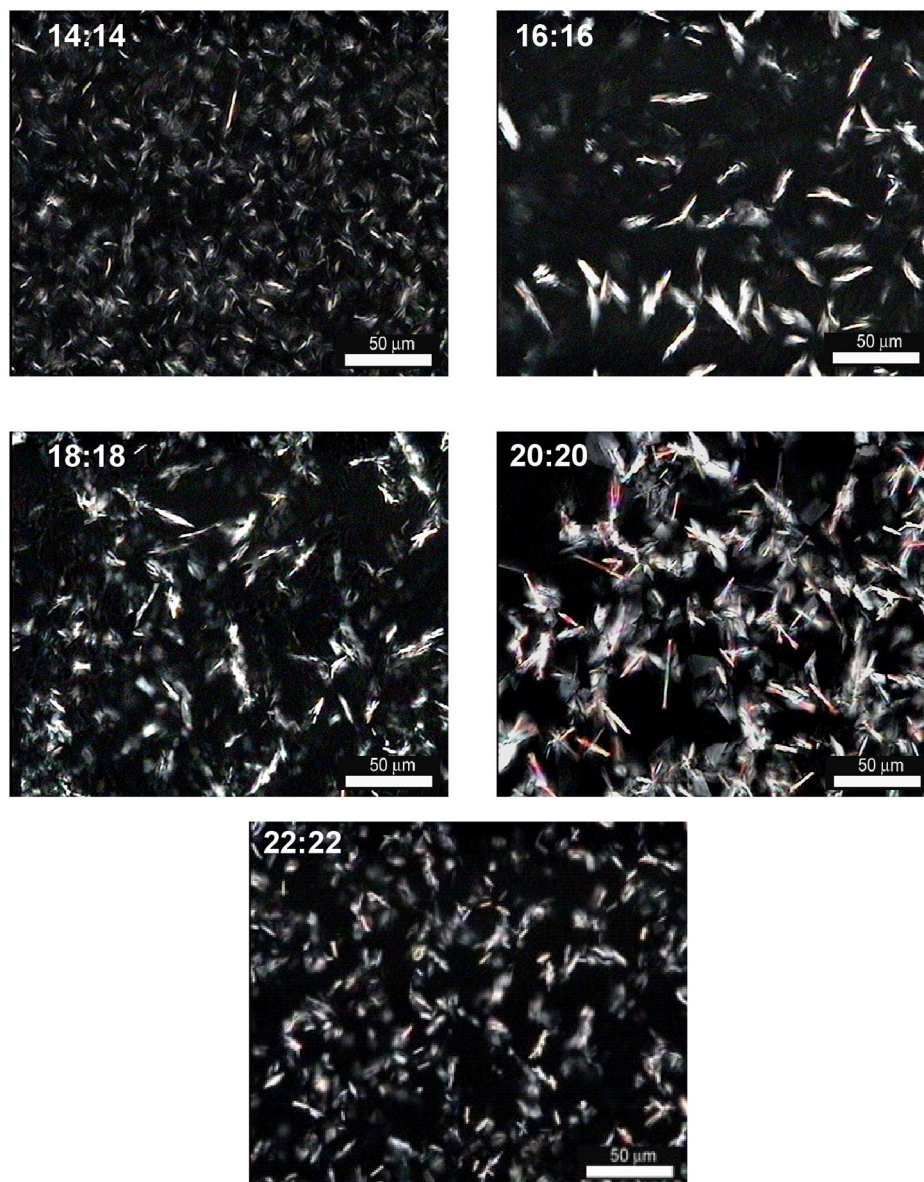


FIGURE 6 | Polarized light microscopy (-5°C) for the 3% (wt/wt) oleogels in high oleic safflower oil formulated with the symmetric alkyl esters indicated and 0% MSG.

Nevertheless, in all cases the AE oleogels had higher G' than the SE oleogels, particularly in the presence of MSG (Figures 5B,C). Hwang et al. (2012) reported that wax esters with longer alkyl chains esters required lower quantity to achieve gelation than waxes with shorter alkyl chains. The results in Figure 5A showed that the esters' gelation capability in vegetable oils depends not only on the alkyl chain length, but also on the symmetry or asymmetry of the alkyl chains respect to the ester bond. However, it is important to note that, in contrast with the study of Hwang et al. (2012) that used native waxes (i.e., mixtures of wax esters) containing other additional minor components, the present study used pure saturated alkyl esters. The PLM for the oleogels with 0% MSG showed that, overall, the AE

crystals were larger (Figure 9) than those developed by the SE (Figure 6). Additionally, the AE crystallized in acicular shaped crystals while the SE crystallized mainly as plate-like shaped crystals. This was evident when comparing the PLM of oleogels developed by esters with the same carbon number, i.e., 18:14 and 16:16, and particularly the 18:22 and 20:20 esters (Figures 6, 9). These observations agreed with the microstructure developed by the alkyl esters in the 60% ester solutions previously discussed (Figures 1, 2). For the SE oleogels with 0% MSG the crystals' size increased from the ester with 28 carbons (i.e., 14:14) up to 40 carbons ester (i.e., 20:20). The increase in crystal size resulted in lower extent of crystal-crystal interaction, and therefore in the crystal network's strength. The overall effect was a reduction in

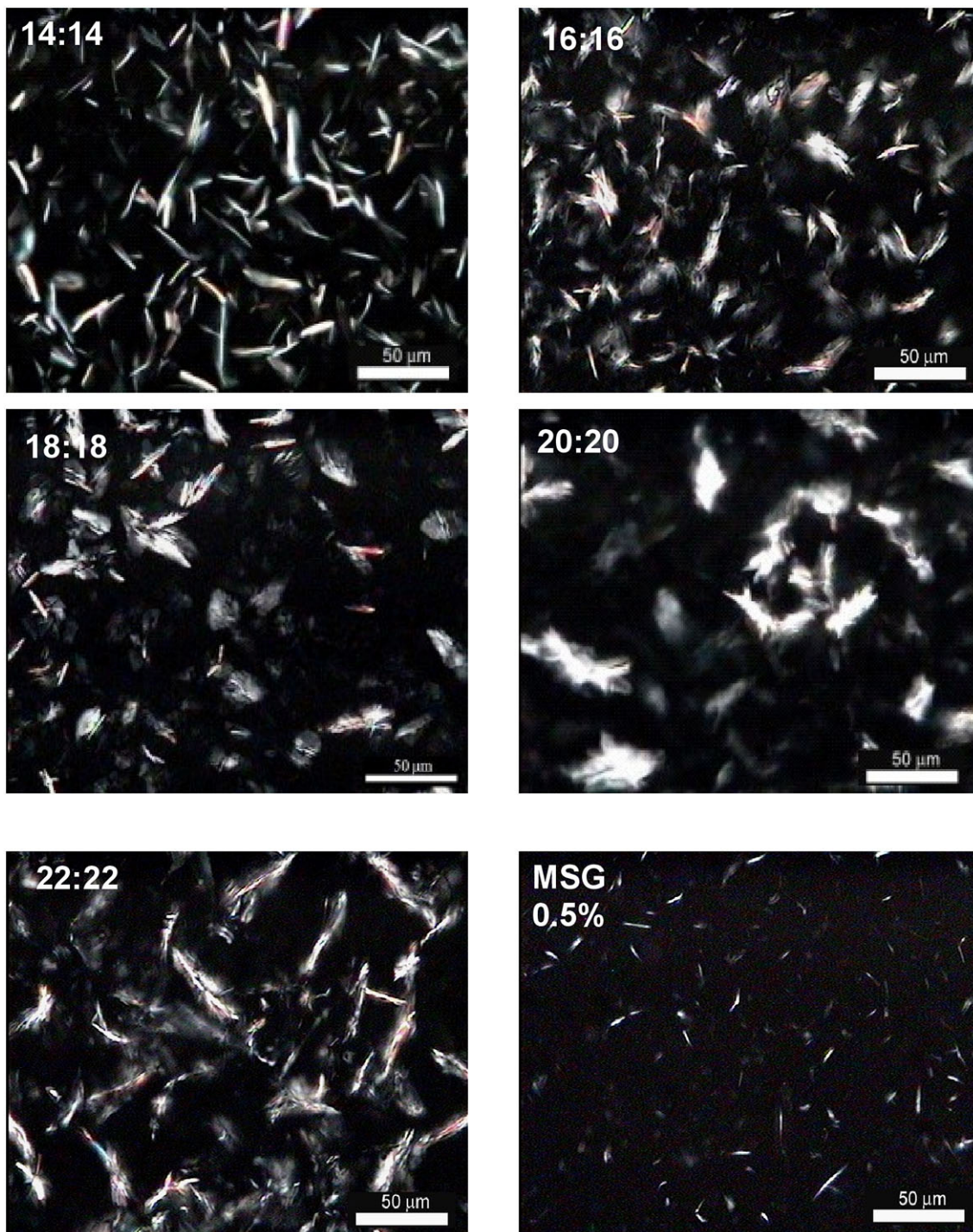


FIGURE 7 | Polarized light microscopy (-5°C) for the 3% (wt/wt) oleogels in high oleic safflower oil formulated with the symmetric alkyl esters indicated and 0.5% MSG.

the elasticity of the SE oleogels as the carbon number increased from 32 (16:16) up to 40 (20:20) (Figures 5A, 6). In contrast, the 22:22 oleogel was structured by smaller crystals (Figure 6) that resulted in an increase in G' . However, the increase in

G' was not statistically different from the elasticity provided by the 20:20 oleogels (Figures 5A, 6). The AE oleogels with 0% MSG also showed an increase in crystal size as the carbon number increased, a behavior associated with the decrease in

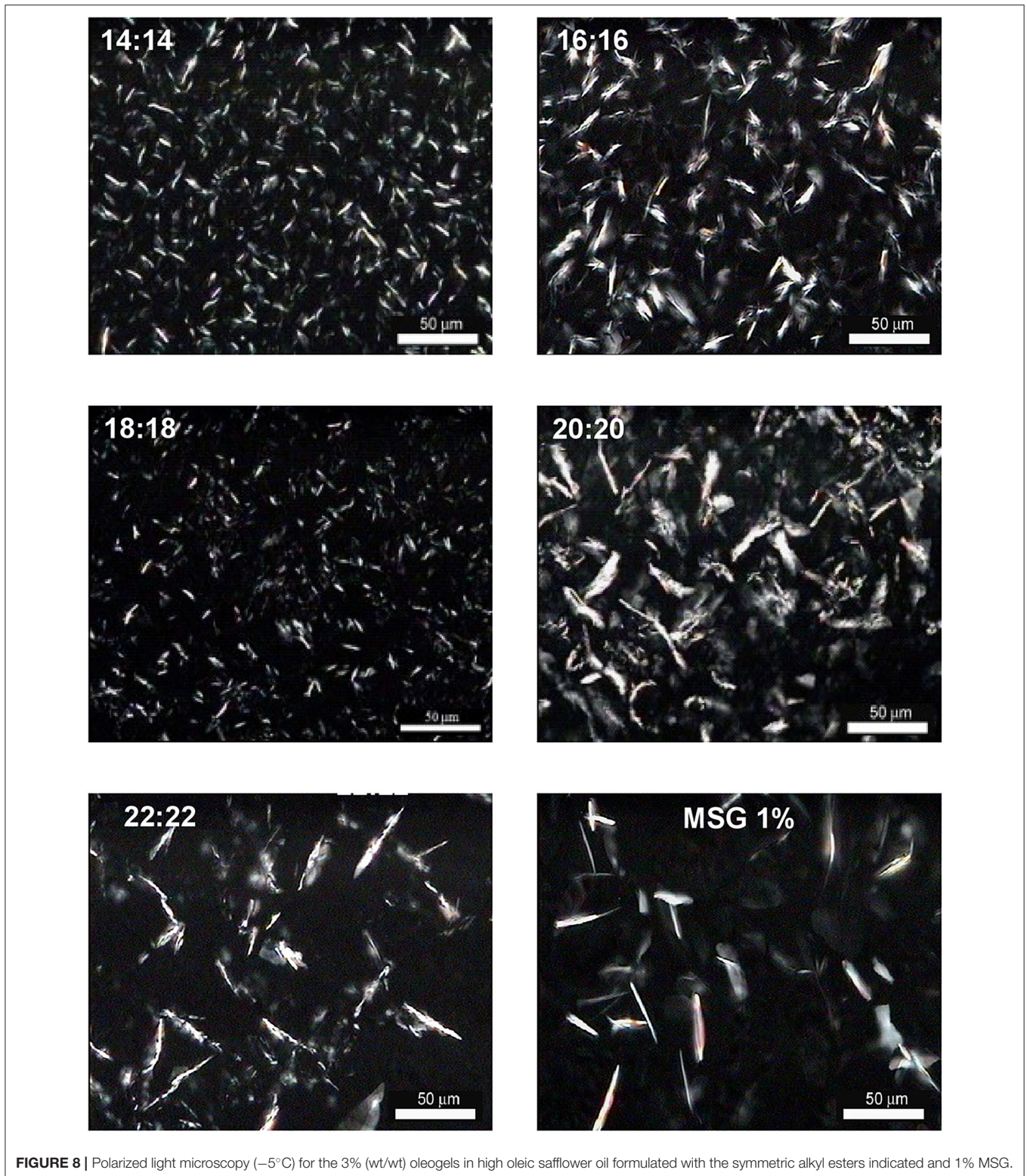


FIGURE 8 | Polarized light microscopy (-5°C) for the 3% (wt/wt) oleogels in high oleic safflower oil formulated with the symmetric alkyl esters indicated and 1% MSG.

the oleogels' elasticity (Figures 5A, 9). The results showed in Figures 5A, 6, 9 indicated that the AE oleogels structured by large acicular crystals (18:14, 18:16, 18:20, and 18:22, Figure 9)

resulted in gels with higher G' when compared with the SE oleogels structured by smaller plate-like crystals (16:16, 18:18, 20:20, and 22:22, Figure 6). Thus, crystal shape in addition to

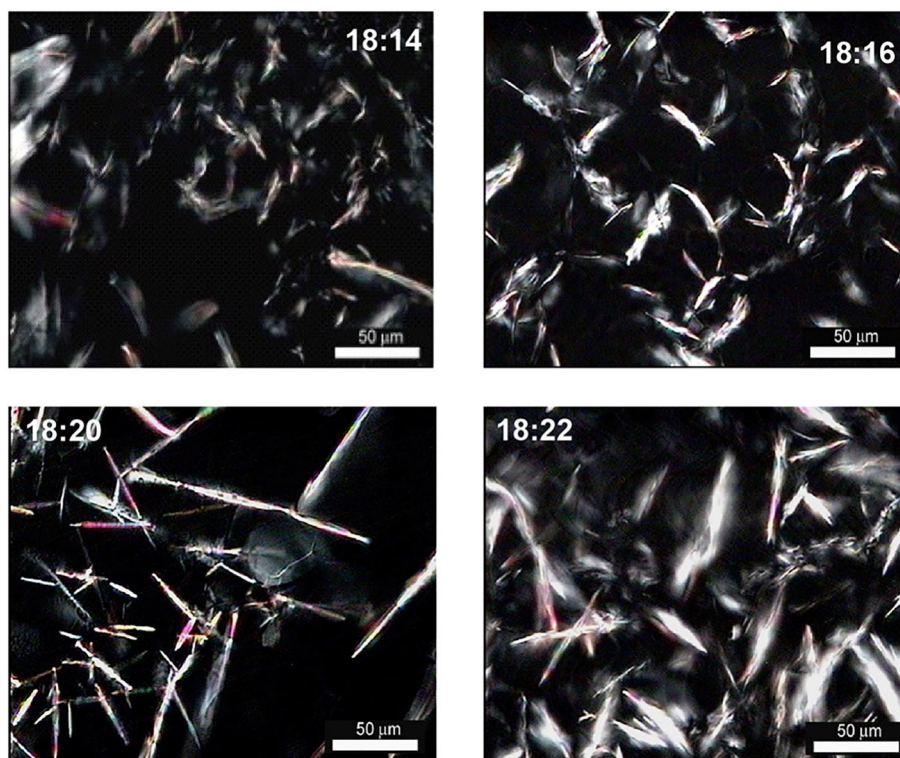


FIGURE 9 | Polarized light microscopy (-5°C) for the 3% (wt/wt) oleogels in high oleic safflower oil formulated with the asymmetric alkyl esters indicated and 0% MSG.

size determined the oleogels rheology. These results agreed with those obtained previously with low molecular weight gelators in the neat state and in oleogels (Toro-Vazquez et al., 2013b). In particular, the 18:22 oleogel was structured by bundles of large fibers (Figure 9) that would increase the crystal-crystal interaction resulting in higher oleogel elasticity than the one achieved by the 20:20 oleogel (Figures 5A, 6). It is important to note that cooling thermograms of the vegetable oil showed that its crystallization onset (i.e., development of a solid phase) occurred between -15°C and -20°C . Additionally, rheological measurements of the vegetable oil under the time-temperature conditions to develop and measure the AE and SE oleogels, showed that G'' was always greater of G' . These results showed that vegetable oil remained liquid at -5°C and therefore its contribution to the oleogels' elasticity was negligible.

Regarding the effect of MSG we noted that the addition of MSG increased the oleogels' elasticity independent of the type of ester and the ester carbon number (Figure 5). However, the MSG effect was higher in the AE oleogels than in the SE oleogels (Figures 5B,C). In particular, the addition of just 0.5% of MSG limited the decrease in G' observed in the oleogels without MSG as the carbon number increased (Figure 5). The addition of MSG had a dramatic effect in the ester's crystal size and shape (Figures 7, 8 for SE; Figures 10, 11 for the AE). This effect was particularly evident in the AE oleogels (compare the photographs of Figure 9 with those in Figures 10, 11). Thus, in comparison with the microstructure of the AE oleogels with 0%

MSG (Figure 9), the addition of just 0.5% MSG to AE oleogels modified the crystal shape and, particularly, decreased the crystal size (Figure 10). However, based on the microphotographs of the oleogels we considered that higher MSG concentrations (i.e., 1% MSG) had no additional effect in the crystal shape and size of the AE (Figure 11). It is important to note that, in comparison with the oleogels with 0% MSG, the addition of MSG ought to result in approximately 0.5 or 1% increase in the oleogels' solid content. Rheological measurements of 0.5 and 1% MSG vegetable oil solutions at -5°C provided G' values of just around 40 Pa or lower, i.e., the solid phase developed by the MSG was not sufficient to form an oleogel. Nevertheless, the increase in the crystal mass (i.e., solid content) and decrease in the crystal size associated with the addition of MSG would result in higher crystal-crystal interaction, and subsequently in higher oleogels' elasticity, particularly in the AE with 38 and 40 carbons (Figure 5).

We did a more detailed rheological analysis of the oleogels by plotting, for the SE and AE oleogels at the different MSG concentrations, the phase angle (δ) as a function of ω (Figures 12, 13). The δ parameter, defined as $\tan^{-1}(G''/G')$, is used to evaluate in a sensitive way the viscoelastic changes occurring in complex systems. Thus, in pure viscous systems, like the vegetable oil, $\delta = 90^{\circ}$ since G'' completely dominates G' . In contrast, $\delta = 0^{\circ}$ in fully structured systems with ideal elastic behavior since G' completely dominates G'' . When the viscous and elastic behavior are exactly balanced $G' = G''$ and, therefore, $\delta = 45^{\circ}$

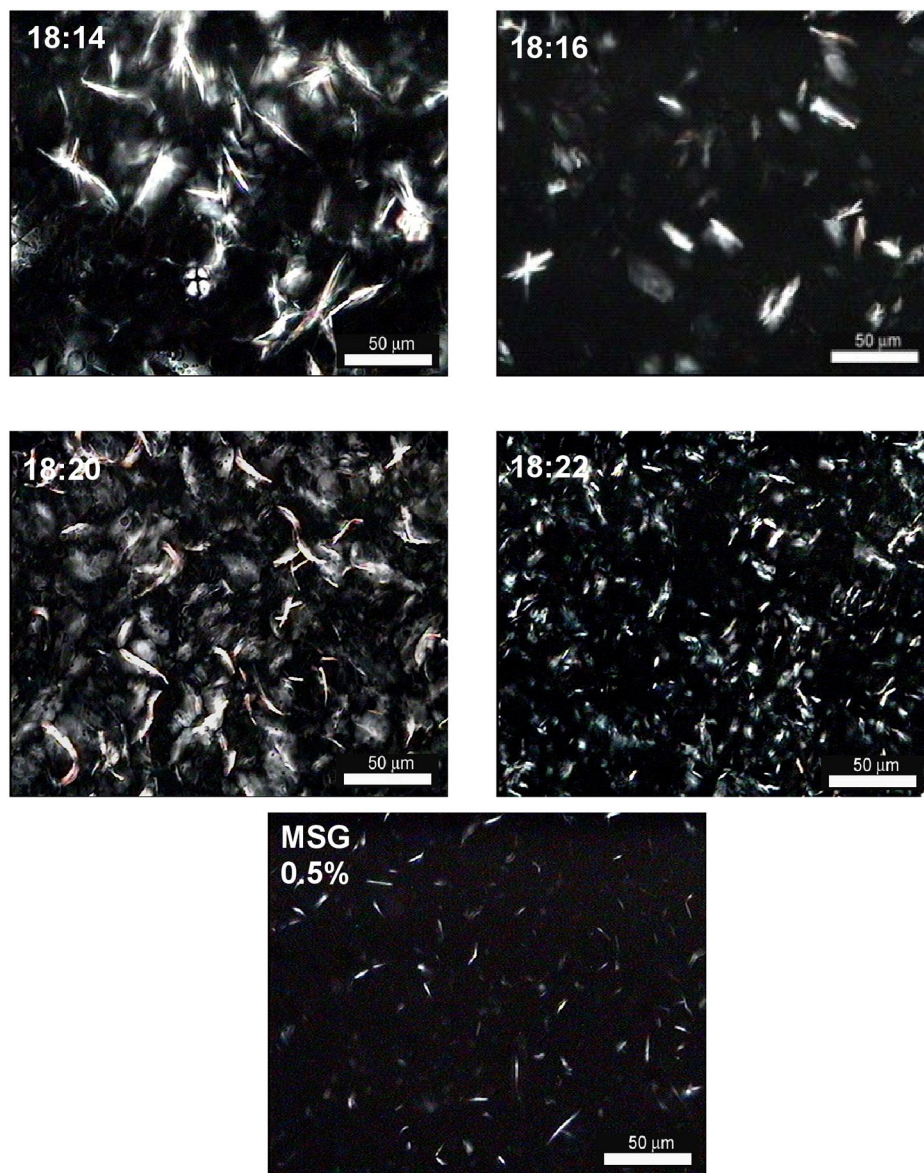


FIGURE 10 | Polarized light microscopy (-5°C) for the 3% (wt/wt) oleogels in high oleic safflower oil formulated with the asymmetric alkyl esters indicated and 0.5% MSG.

(Mezger, 2014). Consequently, in gelled systems (i.e., oleogels) where $G' > G''$ the δ values would be lower than 45° and the smaller the δ value the larger the gel's elasticity. The use of δ sweeps as a function of ω was particularly useful because allows the study of viscoelastic changes occurring as a function of a timescale in complex systems like crystallization of triglycerides or phosphatidylcholine in vegetable or mineral oil (Toro-Vazquez et al., 2005; Martínez-Ávila et al., 2019). Within this context, in solid-like materials δ would have values lower than 45° with a rheological behavior nearly independent of δ (i.e., true gels). In contrast, the more δ behaves ω dependent showing values above 45° the more fluid like is the material (i.e., a sol or a gel-like material). Thus, except the 16:16 oleogel, the ω sweeps of

the SE oleogels with 0% MSG showed δ values above 20° . In particular, the 14:14 and 18:18 oleogels with 0% MSG observed a frequency independent rheological behavior at a $\omega < 15$ Hz with δ values between 30° and 40° . However, at higher ω the δ values increased up to values between 75° and 80° (Figure 12A). In contrast, below 1.5 Hz the 20:20 oleogel with 0% MSG showed δ values that varied between 20° and 50° , while the 22:22 oleogel had δ values between 20° and 35° . Thus, below 1.5 Hz the 20:20 and 22:22 oleogels with 0% MSG showed frequency dependent rheological behavior that further continued at higher ω until δ achieved values around 50° to 55° . These results showed that the 14:14, 18:18, 20:20 and the 22:22 oleogels with 0% MSG were weak gels that would go through phase separation

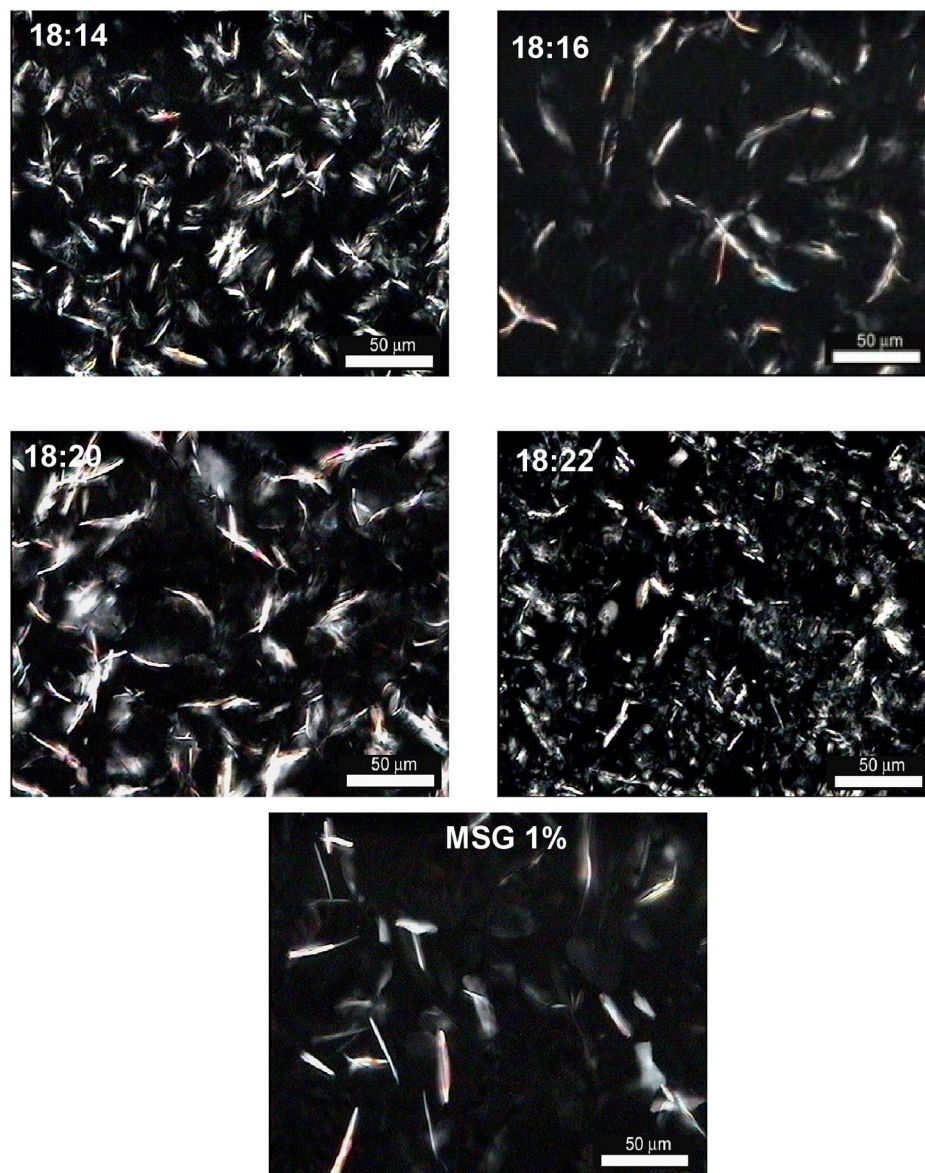


FIGURE 11 | Polarized light microscopy (-5°C) for the 3% (wt/wt) oleogels in high oleic safflower oil formulated with the asymmetric alkyl esters indicated and 1% MSG.

during storage. In fact these oleogels showed some visual phase separation after about four to six weeks of storage at -5°C . The exception to this behavior was the 16:16 oleogel with 0% MSG. This oleogel showed essentially a frequency independent rheological behavior in most of the ω interval, providing δ values around 16° (Figure 12A). Thus, the 16:16 oleogels with 0% MSG showed the rheological behavior of a true gel. However, the 16:16 oleogels' rheological behavior could not be explained considering just the oleogels' microstructure (Figure 6). In contrast, the AE oleogels with 0% MSG had δ values well below 35° showing essentially a frequency independent rheological behavior. At ω higher than 0.3 Hz the AE oleogels with 0% MSG had a tendency of achieving lower δ values (i.e., higher elasticity) as the carbon

number decreased from 18:22 ($\delta \approx 20^{\circ}$ to 29°) to 18:14 ($\delta \approx 6^{\circ}$ to 10°) (Figure 13A). Thus, in contrast with the SE oleogels with 0% MSG all the AE oleogels with 0% MSG showed the rheological behavior of a true gel. Within this context it is important to point out that for the same carbon number, the AE oleogels (i.e., 18:14, 18:22) had significantly lower δ values (i.e., higher elasticity) than the corresponding SE oleogels (i.e., 16:16, 20:20) (Figures 12A, 13A). The difference in rheological behavior between the SE and AE oleogels with 0% MSG was explained considering the oleogels microstructure previously discussed (Figures 6, 9) and its effect in the crystal-crystal interaction and therefore in the oleogels elasticity. Nevertheless, as previously indicated, the 16:16 oleogel with 0% MSG was the only SE that showed a ω independent

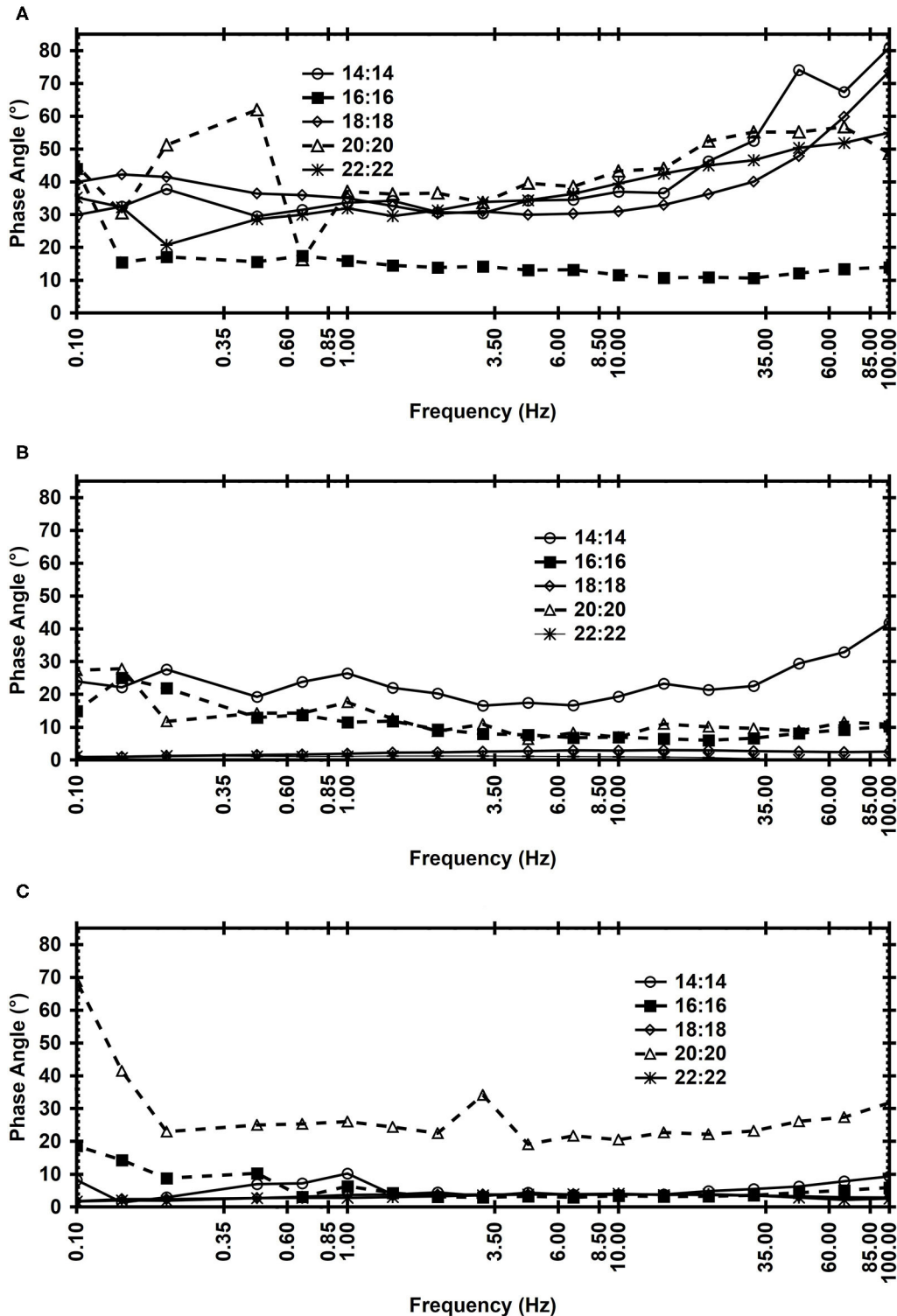


FIGURE 12 | Frequency sweeps (-5°C) for the 3% (wt/wt) oleogels in high oleic safflower oil formulated with the symmetric alkyl esters indicated and: 0% MSG (A), 0.5% MSG (B), and 1% MSG (C).

rheological behavior as the AE oleogels (Figures 12A, 13A). The 16:16 oleogel had a microstructure closer to that developed by the AE oleogels (Figures 6, 9), and possible this was the reason the

16:16 oleogel showed similar ω independent rheological behavior as the AE oleogels. Within this context, as previously noted, the neat 16:16 was the only SE that showed a similar X-ray diffraction

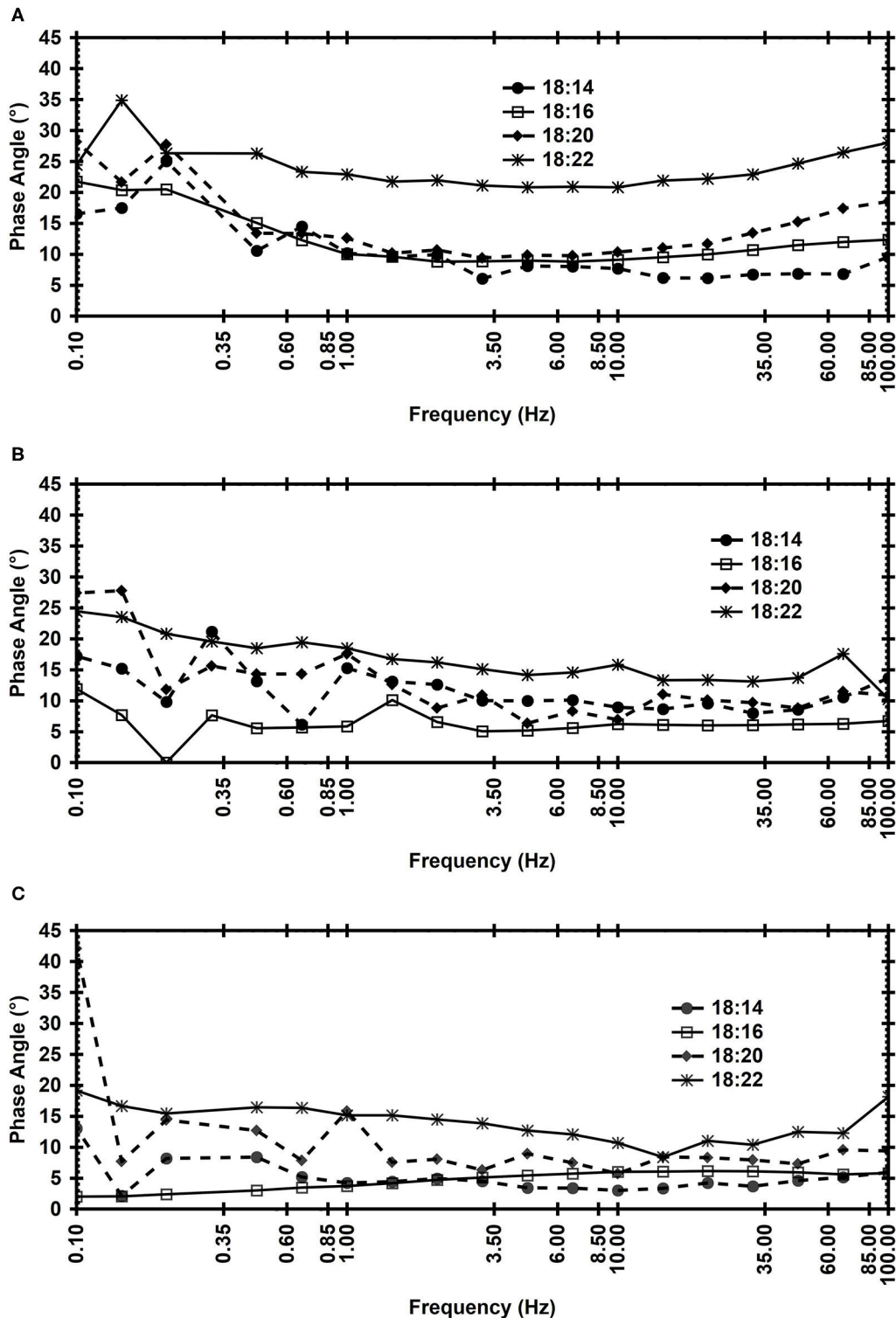


FIGURE 13 | Frequency sweeps (-5°C) for the 3% (wt/wt) oleogels in high oleic safflower oil formulated with the asymmetric alkyl esters indicated and: 0% MSG (A), 0.5% MSG (B), and 1% MSG (C).

pattern to neat AE. Thus, like the neat AE the X-ray diffraction for 16:16 showed a lower diffraction signal in the WAXS region than in the SAXS region. Unfortunately, we could not find

the reasons why the particular crystallization and rheological behavior of the 16:16 ester in the neat state and the oleogel. We did not consider that the rheological behavior showed by the AE

and SE oleogels with 0% MSG was associated with differences in the oleogels' solid content. As already discussed, at the gel setting temperature used for rheological measurements (-5°C), we assured the complete crystallization of all the alkyl esters (i.e., 3%). Thus, cooling thermograms of the 3% alkyl esters solutions in the vegetable oil showed that the corresponding crystallization exotherm ended at a temperature well above the gel setting temperature (from -1.7°C for the 14:14 oleogel up to 37.2°C for the 22:22 oleogel). Unfortunately, due to the limited amount of pure esters available we could not determine the oleogels' solid content. Therefore, the rheological behavior of the SE and AE oleogels with 0% MSG was mainly associated with the microstructural organization of the alkyl esters in the oleogels (Figures 6, 9).

On the other hand, independent of the type of ester, the addition of 0.5% MSG and particularly 1% MSG resulted in gels that provided lower δ values (Figures 12B,C, 13B,C) and, therefore, better structured than the oleogels with 0% MSG (Figures 12A, 13A). Except the δ behavior observed by the 18:20 and 20:20 oleogels with 1% MSG at ω lower than 0.30 Hz (Figures 12C, 13C), and the 14:14 oleogel with 0.5% MSG at ω above 50 Hz (Figure 12B), all the AE and SE oleogels with 0.5% or 1% MSG showed δ values lower than 30° with ω independent rheological behavior (Figures 12B,C, 13B,C). In contrast with the oleogels with 0% MSG, we considered that the rheological behaviors of the SE and AE oleogels with 0.5% and 1% MSG were associated with the microstructural organization of the oleogels previously discussed (Figures 7, 8 for the SE, and Figures 10, 11 for the AE), but also with the higher solid content associated with the MSG crystallization. Other studies had shown that the presence of minor components of vegetable oils (i.e., tripalmitin) have a profound effect in the gelation capability and the molecular self-assembly mechanism of the hentriacontane (i.e., *n*-alkane with 31 carbons) present in candelilla wax (Morales-Rueda et al., 2009; Chopin-Doroteo et al., 2011). As previously discussed, we observed that a small amount of MSG modified the crystal habit of neat alkyl esters (Figures 7, 8), developing oleogels with higher elasticity than the ester oleogels (Figures 5B,C). As examples, the Figures 8SM, 9SM of the Supplementary Material show cooling and heating thermograms for a symmetrical (i.e., 18:18) and asymmetrical (i.e., 18:16) oleogels with 0.5 and 1% MSG, in comparison with the corresponding independent systems, i.e., the 3% alkyl ester oleogel and the corresponding 0.5 and 1% MSG solution in the vegetable oil. The photographs for these oleogels obtained at -5°C through PLM are included in the Figures 8SM, 9SM. We noted that the crystallization and further melting of the MSG in the corresponding 0.5 and 1% solutions were modified when occurred in the alkyl ester-MSG oleogels. Thus, during cooling and further melting of the independent systems the 3% alkyl esters, the 0.5 and 1% MSG showed exotherms and endotherms of different shapes, T_{Cr} and T_M . However, during cooling of the alkyl ester-0.5% MSG and alkyl ester-1% MSG systems both gelators crystallized showing just one exotherm. Upon heating the oleogels melted showing just one exotherm that, except the 18:18 and 18:22 alkyl esters, had

a T_M statistically equal to the T_M of the corresponding 3% alkyl ester-0% MSG oleogel (see Table 2SM of the Supplementary Material). Within this context, the DSC results of alkyl esters-MSG oleogels suggested that the alkyl ester and the MSG crystallized as one entity, i.e., a co-crystal. It is important to point out that during melting of some of the alkyl ester-MSG oleogels we observed a small shoulder of the major melting endotherm (see arrow in the heating thermogram for the 3%18:18-1% MSG oleogel, Figure 8SM panel D). We associated this thermal behavior with the melting of MSG that apparently did not co-crystallize with the alkyl ester during cooling. This might be the reason why the 18:18 and 18:22 alkyl esters oleogels with 0.5 and 1% MSG showed an endotherm with a higher T_M than the corresponding alkyl esters oleogels with 0% MSG ($P < 0.05$; Table 2SM of the Supplementary Material).

The tentative alkyl esters-MSG co-crystals might develop through van der Waals forces established between the hydrocarbon chain of the stearic acid esterified to the MSG and the alkyl chains of the AE or SE. This would result in a modification of the original ester self-assembly and, subsequently, in the crystal size and shape. The calorimetry results also showed that in alkyl ester-MSG oleogels, particularly developed with 1% MSG, part of the MSG did not interact with the ester molecules and crystallized independently of the co-crystals. These MSG crystals might act as active fillers of the major microstructure developed by the alkyl ester-MSG co-crystals. The overall effect was that the alkyl ester-MSG oleogels had higher G' with a δ frequency independent rheological behavior in comparison with the alkyl ester oleogels with 0% (Figures 5, 12, 13).

The results of this study showed that alkyl ester composition and structure (i.e., symmetry or asymmetry) greatly influences its molecular self-assembly, with the consequent effect in the oleogel's thermo-mechanical properties. Additionally, MSG commonly used in the development of organogelled emulsions (Toro-Vazquez et al., 2013a), affected the alkyl ester crystallization resulting in oleogels with higher elastic properties with frequency independent rheological behavior. The rheological properties of the alkyl esters-MSG oleogels were associated with the development of co-crystals between the ester and the monoglyceride. Additionally, part of the MSG that did not interact with the ester molecules and crystallized independently, acted as an active filler of the three-dimensional microstructure formed by the co-crystals. The relevance of these results resides in the major role that alkyl esters play in establishing the functional properties of vegetable wax's oleogels used in food systems and cosmetics. Ongoing studies using molecular mechanics modeling are underway to establish the mechanism for AE and SE self-assembly with and without MSG.

DATA AVAILABILITY STATEMENT

The raw data supporting the conclusions of this article will be made available by the authors, without undue reservation.

AUTHOR CONTRIBUTIONS

GA-V is currently a Ph. D. student and these results are part of her thesis research. GA-V was closely involved in the DSC, rheological measurements and implementing the microscopy technique to evaluate the crystallization of the esters in the neat state and in the oleogels. AD and MEC-A were mainly involved in doing the X-ray analysis and their diffractograms interpretation within the context of the symmetrical and asymmetrical ester molecular self-assembly. MAC-A and JT-V established the experimental conditions used in this study, integrated and analyzed all data. AD, MAC-A, and JT-V obtained and analyze the data associated with the Hildebrand equation applied to the crystallization and melting behavior of the ester in vegetable oil solutions. JT-V was the project and research group leader, also

acting as GA-V's thesis advisor. All authors contributed to the article and approved the submitted version.

ACKNOWLEDGMENTS

The present research was supported by Consejo Nacional de Ciencia y Tecnología (CONACYT) through the Grant No. CB-280981-2018. GA-V greatly appreciates the scholarship provided by CONACYT to conclude her Ph.D. program. The technical support from Marisol Davila Martínez is greatly appreciated.

SUPPLEMENTARY MATERIAL

The Supplementary Material for this article can be found online at: <https://www.frontiersin.org/articles/10.3389/fsufs.2020.00132/full#supplementary-material>

REFERENCES

- Abdallah, D. J., and Weiss, R. G. (2000). n-Alkanes gel n-alkanes (and many other organic liquids). *Langmuir* 16, 352–355. doi: 10.1021/la990795r
- Abraham, S., Lan, Y., Lam, R. S. H., Grahame, D. A. S., Kim, J. J. H., Weiss, R. G., et al. (2012). Influence of positional isomers on the macroscale and nanoscale architectures of aggregates of racemic hydroxyoctadecanoic acids in their molecular gel, dispersion, and solid states. *Langmuir* 28, 4955–4964. doi: 10.1021/la204412t
- Alvarez-Mitre, F. M., Morales-Rueda, J. A., Dibildox-Alvarado, E., Charó-Alonso, M. A., and Toro-Vazquez, J. F. (2012). Shearing as a variable to engineer the rheology of candelilla wax organogels. *Food Res. Intern.* 49, 580–587. doi: 10.1016/j.foodres.2012.08.025
- Blake, A. I., Co, E., and Marangoni, A. G. (2014). Structure and physical properties of plant wax crystal networks and their relationship to oil binding capacity. *J. Am. Oil Chem. Soc.* 91, 885–903. doi: 10.1007/s11746-014-2435-0
- Blake, A. I., Toro-Vazquez, J. F., and Hwang, H.-S. (2018). “Wax oleogels,” in *Edible Oleogels. Structure and Health Implications*, eds G. Alejandro, M. Nissim Garti (San Diego, CA: AOCs Press), 133–171. doi: 10.1016/B978-0-12-814270-7.00006-X
- Boese, R., Weiss, H. C., and Bläser, D. (1999). The melting point alternation in the short-chain n-alkanes: Single-crystal X-ray analyses of propane at 30 K and of n-butane to n-nonane at 90 K. *Angew. Chem. Intern. Edn.* 38, 988–992.
- Bot, A., and Agerof, W. G. M. (2006). Structuring of edible oils by mixtures of γ -oryzanol with β -sitosterol or related phytosterols. *J. Am. Oil Chem. Soc.* 83, 513–521. doi: 10.1007/s11746-006-1234-7
- Bot, A., Den Adel, R., and Roijers, E. C. (2008). Fibrils of γ -oryzanol + β -sitosterol in edible oil organogels. *J. Am. Oil Chem. Soc.* 85, 1127–1134. doi: 10.1007/s11746-008-1298-7
- Bot, A., den Adel, R., Roijers, E. C., and Regkos, C. (2009). Effect of sterol type on structure of tubules in sterol + γ -oryzanol-based organogels. *Food Biophys.* 4, 266–272. doi: 10.1007/s11483-009-9124-9
- Busson-Breyse, J., Farines, M., and Soulier, J. (1994). Jojoba wax: its esters and some of its minor components. *J. Am. Oil Chem. Soc.* 71, 999–1002. doi: 10.1007/BF02542268
- Chen, C. H., Damme, I. V., and Terentjev, E. M. (2009). Phase behavior of C18 monoglyceride in hydrophobic solutions. 432–439. doi: 10.1039/B813216j
- Chopin-Doroteo, M., Morales-Rueda, J. A., Dibildox-Alvarado, E., Charó-Alonso, M. A., de la Peña-Gil, A., Jorge, F., et al. (2011). The effect of shearing in the thermo-mechanical properties of candelilla wax and candelilla wax-tripalmitin organogels. *Food Biophys.* 6, 359–376. doi: 10.1007/s11483-011-9212-5
- Co, E., and Marangoni, A. G. (2012). Organogels: An alternative edible oil-structuring method. *J. Am. Oil Chem. Soc.* 89, 749–780. doi: 10.1007/s11746-012-2049-3
- Co, E., and Marangoni, A. G. (2013). The formation of a 12-hydroxystearic acid/vegetable oil organogel under shear and thermal fields. *J. Am. Oil Chem. Soc.* 90, 529–544. doi: 10.1007/s11746-012-2196-6
- Cosmetic Lab, S. C. (2016). *9 Most Important Natural Waxes For Cosmetics (Part II)*. Available online at: <https://skinchakra.eu/blog/archives/411-9-most-important-natural-waxes-for-cosmetics-Part-II.html> (accessed February 20 2019).
- Dassanayake, L. S. K., Kodali, D. R., and Ueno, S. (2011). Formation of oleogels based on edible lipid materials. *Curr. Opin. Coll. Interf. Sci.* 16, 432–439. doi: 10.1016/j.cocis.2011.05.005
- Dassanayake, L. S. K., Kodali, D. R., Ueno, S., and Sato, K. (2009). Physical properties of rice bran wax in bulk and organogels. *J. Am. Oil Chem. Soc.* 86, 1163–1173. doi: 10.1007/s11746-009-1464-6
- Doan, C. D., To, C. M., De Vrieze, M., Lynen, F., Danthine, S., Brown, A., et al. (2017). Chemical profiling of the major components in natural waxes to elucidate their role in liquid oil structuring. *Food Chem.* 214, 717–725. doi: 10.1016/j.foodchem.2016.07.123
- Ferrari, V., and Mondet, J. (2003). *Inventor; L'Oreal S. A., assignee. Care and/or Make-Up Cosmetic Composition Structured with Silicone Polymers and Organogelling Agents, in Rigid Form*. International WO/2003/105788. Available online at: <https://patentscope.wipo.int/search/en/detail.jsf?docId=WO2003105788>
- Fórmula Botánica (2019). *6 Vegan Waxes for Organic Cosmetic Formulations*. Available online at: <https://formulabotanica.com/6-vegan-waxes/> (accessed February 20 2019)
- Gandolfo, F. G., Bot, A., and Flöter, E. (2004). Structuring of edible oils by long-chain fa, fatty alcohols, and their mixtures. *J. Am. Oil Chem. Soc.* 81, 1–6. doi: 10.1007/s11746-004-0851-5
- Ghamdi, A. K., Al, E.lkholy, T. A., Abuhelal, S., Alabbadi, H., Qahwaji, D., Sobhy, H., et al. (2017). Study of Jojoba (*Simmondsia chinensis*) oil by gas chromatography. *Nat. Prod. Chem. Res.* 05:283. doi: 10.4172/2329-6836.1000283
- Gunstone, F. D. (2002). *Vegetable Oils in Food Technology: Composition, Properties, and Uses*. Copenhagen: Blackwell Publishing Ltd.
- Han, L., Li, L., Li, B., Zhao, L., Liu, G. Q., Liu, X., et al. (2014). Structure and physical properties of organogels developed by sitosterol and lecithin with sunflower oil. *J. Am. Oil Chem. Soc.* 91, 1783–1792. doi: 10.1007/s11746-014-2526-y
- Hildebrand, J. H., and Robert-Lane, S. (1950). *The Solubility of Nonelectrolytes (3rd edn)*. New York, N.Y.: Reinhold.
- Hwang, H. S., Sanghoon, K., Mukti, S., Jill, K. W. M., and Liu, S. X. (2012). Organogel formation of soybean oil with waxes. *J. Am. Oil Chem. Soc.* 89, 639–647. doi: 10.1007/s11746-011-1953-2
- Hwang, H. S., Singh, M., Winkler-Moser, J. K., Bakota, E. L., and Liu, S. X. (2014). Preparation of margarines from organogels of sunflower wax and vegetable oils. *J. Food Sci.* 79, C1926–C1932. doi: 10.1111/1750-3841.12596
- Lam, R. S. H., and Rogers, M. A. (2011). Activation energy of crystallization for trihydroxystearin, stearic acid, and 12-hydroxystearic acid under nonisothermal cooling conditions. *Crystal Growth Design* 11, 3593–3599. doi: 10.1021/cg200553t

- López-Martínez, A., Morales-Rueda, J. A., Dibildox-Alvarado, E., Charó-Alonso, M. A., Marangoni, A. G., and Toro-Vazquez, J. F. (2014). Comparing the crystallization and rheological behavior of organogels developed by pure and commercial monoglycerides in vegetable oil. *Food Research Intern.* 64, 946–957. doi: 10.1016/j.foodres.2014.08.029
- Marangoni, A. G., and Garti, N. (2011). *Edible Oleogels Structure and Health Implications*. Indiana, IL: AOCS Press.
- Marangoni, A. G., and Garti, N. (2018). *Edible Oleogels Structure and Health Implications. 2nd Edn*. Indiana, IL: AOCS Press.
- Martínez-Ávila, M., De la Peña-Gil, A., Álvarez-Mitre, F. M., Charó-Alonso, M. A., and Toro-Vazquez, J. F. (2019). Self-assembly of saturated and unsaturated phosphatidylcholine in mineral and vegetable oils. *J. Am. Oil Chem. Soc.* 96, 273–289. doi: 10.1002/aocs.12188
- McGann, M. R., and Lacks, D. J. (1999). Chain length effects on the thermodynamic properties of n-alkane crystals. *J. Phys. Chem. B* 103, 2796–2802. doi: 10.1021/jp983932m
- Mezger, T. G. (2014). *The Rheology Handbook: For Users of Rotational and Oscillatory Rheometers (4th edn)*. Hanover: Vincentz Network.
- Morales, M., Gallardo, V., Clarés, B., García, M., and Ruiz, M. (2010). Study and description of hydrogels and organogels as vehicles for cosmetic active ingredients. *J. Cosm. Sci.* 60, 627–636. doi: 10.1111/j.1468-2494.2010.00580_4.x
- Morales-Rueda, J. A., Dibildox-Alvarado, E., Charó-Alonso, M. A., Weiss, R. G., and Toro-Vazquez, J. F. (2009). Thermo-mechanical properties of candelilla wax and dotriacontane organogels in safflower oil. *Eur. J. Lipid Sci. Technol.* 111, 207–215. doi: 10.1002/ejlt.200810174
- Ojijo, N. K. O., Neeman, L., Eger, S., and Shimoni, E. (2004). Effects of monoglyceride content, cooling rate and shear on the rheological properties of olive oil/monoglyceride gel networks. *J. Sci. Food Agric.* 84, 1585–1593. doi: 10.1002/jsfa.1831
- Pal, A., Shibu, A., Michael, A. R., Joykrishna, D., and Richard, G. W. (2013). Comparison of dipolar, H-bonding, and dispersive interactions on gelation efficiency of positional isomers of keto and hydroxy substituted octadecanoic acids. *Langmuir* 29, 6467–6475. doi: 10.1021/la400664q
- Patel, A. R., Bahaahmadi, M., Lesaffer, A., and Dewettinck, K. (2015). Rheological profiling of organogels prepared at critical gelling concentrations of natural waxes in a triacylglycerol solvent. *J. Agric. Food Chem.* 63, 4862–4869. doi: 10.1021/acs.jafc.5b01548
- Perez-Nowak, V. (2012). *Inventor; L'Oreal, S. A., Assignee. Fluid Cosmetic Composition, Useful for Making Up and/or Caring the Skin and/or Lips, Comprises Polyester, Non-Volatile Silicone Oil, Organogelling Agent Comprising N-Acylglutamides e.g. N-Lauroylglutamic Acid Dibutylamide, and Wax*. France patent FR2975296A1 (2012). Available online at: <https://patents.google.com/patent/FR2975296A1/en?q=FR+Patent+2975296+A1>
- Rocha-Amador, O. G., Gallegos-Infante, J. A., Huang, Q., Rocha-Guzman, N. E., Rociomoren Jimenez, M., and Gonzalez-Laredo, R. F. (2014). Influence of commercial saturated monoglyceride, mono-/diglycerides mixtures, vegetable oil, stirring speed, and temperature on the physical properties of organogels. *Intern. J. Food Sci.* 1–8. doi: 10.1155/2014/513641
- Rogers, M. A., and Marangoni, A. G. (2008). Non-isothermal nucleation and crystallization of 12-hydroxystearic acid in vegetable oils. *Crys. Growth Design* 8, 4596–4601. doi: 10.1021/cg8008927
- Rogers, M. A., Strober, T., Bot, A., Toro-Vazquez, J. F., Stortz, T., and Marangoni, A. G. (2014). Edible oleogels in molecular gastronomy. *Intern. J. Gastron. Food Sci.* 2, 22–31. doi: 10.1016/j.ijgfs.2014.05.001
- Sagiri, S. S., Singh, V. K., Pal, K., Banerjee, I., and Basak, P. (2015). Stearic acid based oleogels: A study on the molecular, thermal and mechanical properties. *Mater. Sci. Eng. C* 48, 688–699. doi: 10.1016/j.msec.2014.12.018
- Toro-Vazquez, J. F., Mauricio-Pérez, R., González-Chávez, M. M., Sánchez-Becerril, M., Ornelas-Paz, J., de, J., et al. (2013a). Physical properties of organogels and water in oil emulsions structured by mixtures of candelilla wax and monoglycerides. *Food Res. Intern.* 54, 1360–1368. doi: 10.1016/j.foodres.2013.09.046
- Toro-Vazquez, J. F., Morales-Rueda, J., Torres-Martínez, A., Charó-Alonso, M. A., Mallia, V. A., and Weiss, R. G. (2013b). Cooling rate effects on the microstructure, solid content, and rheological properties of organogels of amides derived from stearic and (R)-12-hydroxystearic acid in vegetable oil. *Langmuir* 29, 7642–7654. doi: 10.1021/la400809a
- Toro-Vazquez, J. F., Morales-Rueda, J. A., Dibildox-Alvarado, E., Charó-Alonso, M. A., Alonzo-Macias, M., and González-Chávez, M. M. (2007). Thermal and textural properties of organogels developed by candelilla wax in safflower oil. *J. Am. Oil Chem. Soc.* 84, 989–1000. doi: 10.1007/s11746-007-1139-0
- Toro-Vazquez, J. F., and Pérez-Martínez, J. D. (2018). “Thermodynamic aspects of molecular gels,” in *Monographs in Supramolecular Chemistry*, ed R. G. Weiss (London: Royal Society of Chemistry), 57–87. doi: 10.1039/9781788013147-00057
- Toro-Vazquez, J. F., Rangel-Vargas, E., Dibildox-Alvarado, E., and Charó-Alonso, M. A. (2005). Crystallization of cocoa butter with and without polar lipids evaluated by rheometry, calorimetry and polarized light microscopy. *Eur. J. Lipid Sci. Technol.* 107, 641–655. doi: 10.1002/ejlt.200501163

Conflict of Interest: The authors declare that the research was conducted in the absence of any commercial or financial relationships that could be construed as a potential conflict of interest.

Copyright © 2020 Avendaño-Vázquez, De la Peña-Gil, Charó-Alvarado, Charó-Alonso and Toro-Vazquez. This is an open-access article distributed under the terms of the Creative Commons Attribution License (CC BY). The use, distribution or reproduction in other forums is permitted, provided the original author(s) and the copyright owner(s) are credited and that the original publication in this journal is cited, in accordance with accepted academic practice. No use, distribution or reproduction is permitted which does not comply with these terms.